RESEARCH NOTE

Genomewide association study identifies no major founder variant in Caucasian moyamoya disease

WANYANG LIU[1,7], S. T. M. L. D. SENEVIRATHNA[1], TOSHIAKI HITOMI[1], HATASU KOBAYASHI[1], CONSTANTIN RODER[2], ROMAN HERZIG[3], MARKUS KRAEMER[4], MAURITS H. J. VOORMOLEN[5], PAVLÍNA CAHOVÁ[6], BORIS KRISCHEK[2*] and AKIO KOIZUMI[1*]

[1]*Department of Health and Environmental Sciences, Kyoto University Graduate School of Medicine, Kyoto 606-8501, Japan*
[2]*Department of Neurosurgery, University of Tübingen, Tübingen D-72076, Germany*
[3]*Stroke Comprehensive Center, Department of Neurology, Faculty of Medicine and Dentistry, Palacký University and University Hospital, Olomouc 77900, Czech Republic*
[4]*Department of Neurology, Alfried-Krupp-von Bohlen und Halbach Hospital, Essen 45117, Germany*
[5]*Department of Radiology, Antwerp University Hospital and University of Antwerp, Edegem BE-2000, Belgium*
[6]*Department of Child Neurology, University Hospital, Brno 62500, Czech Republic*
[7]*Department of Nutrition and Food Hygiene, School of Public Health, China Medical University, Shenyang 110001, People's Republic of China*

[Liu W., Senevirathna S. T. M. L. D., Hitomi T., Kobayashi H., Roder C., Herzig R., Kraemer M., Voormolen M. H. J., Cahová P., Krischek B. and Koizumi A. 2013 Genomewide association study identifies no major founder variant in Caucasian moyamoya disease. *J. Genet.* **92**, 605–609]

Introduction

Moyamoya disease (MMD) is an idiopathic cerebrovascular occlusive-stenosis disorder at the terminal portion of internal carotid arteries and its main branches, accompanied by collateral vascular networks at the base of the circle of Willis (Takeuchi and Shimizu 1957; Suzuki and Takaku 1969). MMD has the highest prevalence in East Asian countries and a low prevalence in European countries (Goto and Yonekawa 1992; Kuroda and Houkin 2008). We have found that the p.R4810K variant in the ring finger protein 213 (RNF213) is a major founder susceptibility gene for East Asian MMD (Liu *et al.* 2010, 2011). In this study, we aimed to test whether there is a major founder susceptibility gene for Caucasian MMD using a genomewide association study (GWAS). We demonstrated that there was no major founder variant in Caucasian MMD as it is in East Asian MMD. We identified several suggestive association regions for Caucasian MMD.

*For correspondence. E-mail: Boris Krischek, krischek@gmail.com; Akio Koizumi, koizumi.akio.5v@kyoto-u.ac.jp.
Wanyang Liu and S. T. M. L. D. Senevirathna contributed equally to this work.

Materials and methods

Study subjects

Ethical approval was given by the Institutional Review Boards and Ethics Committees of Kyoto University School of Medicine, Japan; Medical Faculty of the University of Tübingen, Germany; and the Faculty of Medicine and Dentistry of Palacký University, Czech Republic, respectively. Written informed consent was obtained from all participants. We calculated the required size of the study population to obtain enough statistical power in Caucasian population by assuming the following conditions as was reported in East Asian population (Liu *et al.* 2011): the frequency of the high risk allele is 0.01, the prevalence of MMD is $<10^{-4}$; the relative risk of risk allele is 100 by assuming an autosomal dominant mode of inheritance; the marker D' is 0.99 and its frequency >0.05; type I error is 0.05 and statistical power ≥0.8 (http://pngu.mgh.harvard.edu/~purcell/gpc/). The calculation indicated that 40 for cases and controls can assure the statistical power of 0.8. Cases are composed of 38 unrelated subjects: seven were Czech and 31 were German. Those cases were case-series patients between February 2008 and November 2009 in participating hospitals. Controls were all unrelated Germans, in whom, absence of MMD were confirmed by magnetic resonance imaging (MRI) in the same period.

Keywords. Caucasian; founder variant; genomewide association study; moyamoya disease; suggestive association.

DNA isolation, genotyping and quality control

Genomic DNA was extracted from the blood samples using a QIAamp DNA Blood Mini Kit (Qiagen, Germantown, USA) according to the manufacturer's protocol. Genomewide genotyping was performed using an Illumina Human610-Quad BeadChip Kit (Illumina, San Diego, USA). Samples with overall call rates <95% were excluded. Single nucleotide polymorphisms (SNPs) that met the following criteria were excluded: had call rates <0.99 in all GWAS samples and genotype distributions deviated from those expected by Hardy–Weinberg equilibrium (HWE). Principal component analysis showed no outliers or population stratification, and all subjects were confirmed to be of Caucasian ethnicity (see figure 1 in electronic supplementary material at http://www.ias.ac.in/jgenet/). A quantile–quantile plot revealed that the distribution of observed P values followed the expected distribution (see figure 2 in electronic supplementary material). After quality control, 565,294 out of 620,901 SNPs for the 38 cases and 41 controls were retained for GWAS.

Candidate genes sequencing by the Sanger method

Five cases and one control were randomly selected for sequencing of all coding exons and at least 100-bp exon–intronic boundaries in eight candidate genes from within five suggestive association regions for the case–control study. The primers that were used for direct sequencing are shown in table 1 in electronic supplementary material. The sequencing products were separated on an ABI Prism 3100 Avant DNA sequencer (Applied Biosystems, Kyoto, Japan). In addition, we investigated the association of SNPs in known two genes, actin, alpha 2, smooth muscle, aorta (*ACTA2*) (Guo *et al.* 2009) and *RNF213* (Liu *et al.* 2011), with MMD by GWAS.

Statistical analysis

GWAS was conducted using the SNP and Variation Suite V7 (Golden Helix, Bozeman, USA). Thresholds of 5×10^{-8} and 1×10^{-5} were set for genomewide significance and suggestive association, respectively. We assumed that a minor allele frequency of the SNP (i.e., risk marker allele), which is postulated to be the closest marker of the putative moyamoya susceptibility gene, was 0.5 in cases and 0.05 in controls as it does in Japanese population (Liu *et al.* 2011). Under this condition, with the current population sizes for cases and controls, simulation (http://pngu.mgh.harvard.edu/~purcell/gpc/) predicts that 29 out of 38 cases are homozygous or heterozygous for the risk marker allele while four controls were heterozygous for the risk marker allele and 37 controls were homozygous for the wild marker allele. Given an autosomal dominant in HWE, we can expect the odds ratio of the risk marker allele to be 29.8 with $P = 9.53 \times 10^{-10}$. When we assume a more modest condition for an odds ratio of 5, the statistical power was 2×10^{-3} and 215 cases and controls are needed to obtain the SNPs with the genomewide significant P of 5×10^{-8}.

Results

Demographic and clinical profiles of the participants

The participants comprised 38 cases and 41 unrelated controls (see table 2 in electronic supplementary material). The mean age for cases and controls was 31.37 ± 14.83 and 27.34 ± 11.55 years, respectively. The sex ratio of male:female was 14:24 and 8:33 for cases and controls, respectively. Age of onset for the cases was 22.93 ± 16.95 years which indicates that the adult onset was dominant. Cerebral infarction was the major clinical symptom, followed by transient ischemic attack and others. Thirty-five of the cases were diagnosed as bilateral MMD; the other three were unilateral MMD.

Genomewide association study

GWAS was performed under two conditions. One was case–control comparison and the other was cases with and without cerebral infarction comparison. No SNPs reached genomewide significant association under both conditions ($P < 5 \times 10^{-8}$, figure 1). However, GWAS revealed multiple suggestive associations under case–control comparison ($P < 1 \times 10^{-5}$, figures 1a and 2a–d). The top association SNPs were rs1023115 (odds ratio, OR = 6.63, $P = 2.60 \times 10^{-6}$) on 1q23.3, rs11681583 (OR = 6.51, $P = 2.93 \times 10^{-6}$) on 2p22.1, rs3742257 (OR = 0.20, $P = 5.73 \times 10^{-6}$) on 13q14.11, rs2058364 (OR = 5.57, $P = 5.90 \times 10^{-6}$) on 17p13.3 and rs720607 (OR = 0.17, $P = 5.59 \times 10^{-6}$) on 20q13.33 (see table 3 in electronic supplementary material; figure 2, a–d). Under case-only analysis, two SNPs reached genomewide suggestive associations (rs17078141 on 3p22.1, OR = 0.04, $P = 6.10 \times 10^{-6}$; rs2178763 on 4q22.3, OR = 21.81, $P = 6.88 \times 10^{-6}$, table 3 in electronic supplementary material; figures 1b and 2e).

Mutation analysis of candidate genes

Candidate regions covering top suggestive association SNPs were further investigated by direct sequencing (figure 2). There was no annotated gene on 17p13.3 and 4q22.3 that covered rs2058364 and rs2178763, respectively. A summary of the variants detected by direct sequencing is available in table 4 in electronic supplementary material for the case–control study. We identified a total of 79 variants among which five were missense and eight were synonymous; the remaining variants were located in noncoding regions. We considered that synonymous and noncoding variants were unlikely to cause the MMD, even when they have low frequencies in general population. All of the missense variants detected were found in dbSNPs database (http://www.ncbi.nlm.nih.gov/projects/SNP/, NCBI build 36.3). Their allele frequencies in general Caucasian populations were greater than 0.1, suggesting that these missense SNPs were unlikely to be associated with the development of MMD in the Caucasian population. In terms of case-only analysis, four genes (*MYRIP*, *FLJ33065*, *ENTPD3* and *FLJ36665*) were found but no sequence determinations were done.

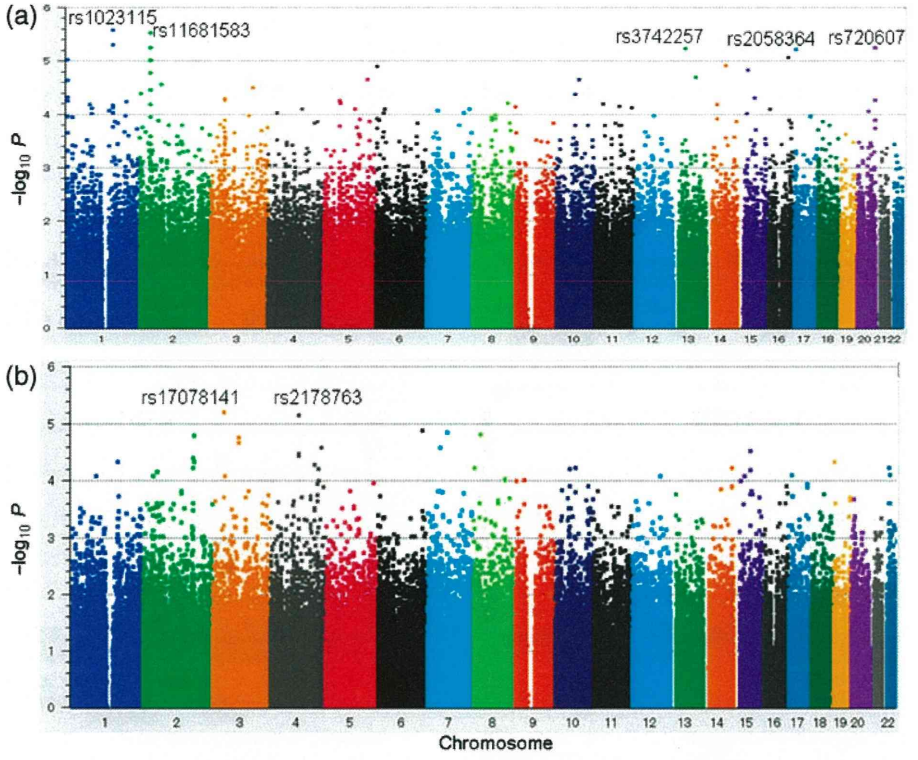

Figure 1. Manhattan plot of the genomewide *P* values of association. The $-\log_{10} P$ values (*y*-axis) are presented against their chromosomal positions (*x*-axis). The top significant associated SNPs are showed. A *P*-value threshold of 1×10^{-5} was taken to represent suggestive association. (a) Analysis for case–control comparison and (b) analysis for case with and without cerebral infarction comparison.

Association with ACTA2 and RNF213

We investigated the association of SNPs in *ACTA2* and *RNF213* with MMD (table 5 in electronic supplementary material). Neither association of SNPs in *ACTA2* nor *RNF213* with MMD was confirmed. However, a cluster of 10 of 25 SNPs in *RNF213* gene region had *P* values less than 0.05, suggesting a possible association with *RNF213* with MMD.

Discussion

We conducted a GWAS to identify the major founder variant for Caucasian MMD but could not find any major founder variant in Caucasian MMD as we did in East Asian MMD. However, we found several suggestive association regions that might be responsible for the Caucasian MMD.

A major founder mutation of p.R4810K in *RNF213* within 17q25.3 was first rigorously identified in East Asian MMD (Liu *et al.* 2011) and perfectly replicated in different cohorts (Miyatake *et al.* 2012; Wu *et al.* 2012). The number of patients with MMD was estimated to be at least 53,800 in East Asian populations (Liu *et al.* 2012). In contrast, we could not detect any founder variants in *RNF213* for Caucasian MMD, suggesting the different genetic background between Caucasian and East Asian MMD. The low prevalence of Caucasian MMD might be due to the lack of the predominant founder variant. However, it should be addressed that there was a cluster of SNPs in *RNF213* region weakly associated with MMD, suggesting *RNF213* as a potential susceptibility gene for MMD even in Caucasian.

Mutations in *ACTA2* were first identified in Caucasian MMD (Guo *et al.* 2009), but they have not been replicated in Japanese and another Caucasian MMD (Shimojima and Yamamoto 2009; Liu *et al.* 2011; Roder *et al.* 2011). We confirmed the absence of association. Importantly, case-only association analysis revealed that *MYRIP* was located around the suggestive association region for cerebral infarction (figures 1b and 2e). *MYRIP* has the highest expression in brain. Fukuda and Kuroda (2002) showed that the C-terminal domain of *MYRIP* directly bound actin, which was encoded by *ACTA2*. The above features suggest that *MYRIP* might be responsible for the progression of MMD in Caucasian population. This observation warrants further investigation in future. The present study, on the other hand, failed to demonstrate the association of SNPs in *RNF213* (see table 5 in electronic supplementary material) with MMD.

This study had several limitations. First, the small number of available samples caused by the rareness of MMD might be the most critical limitation. In this relation, the current study suggests that our study assumption for calculation of statistical power is not realistic. If so, there may be no

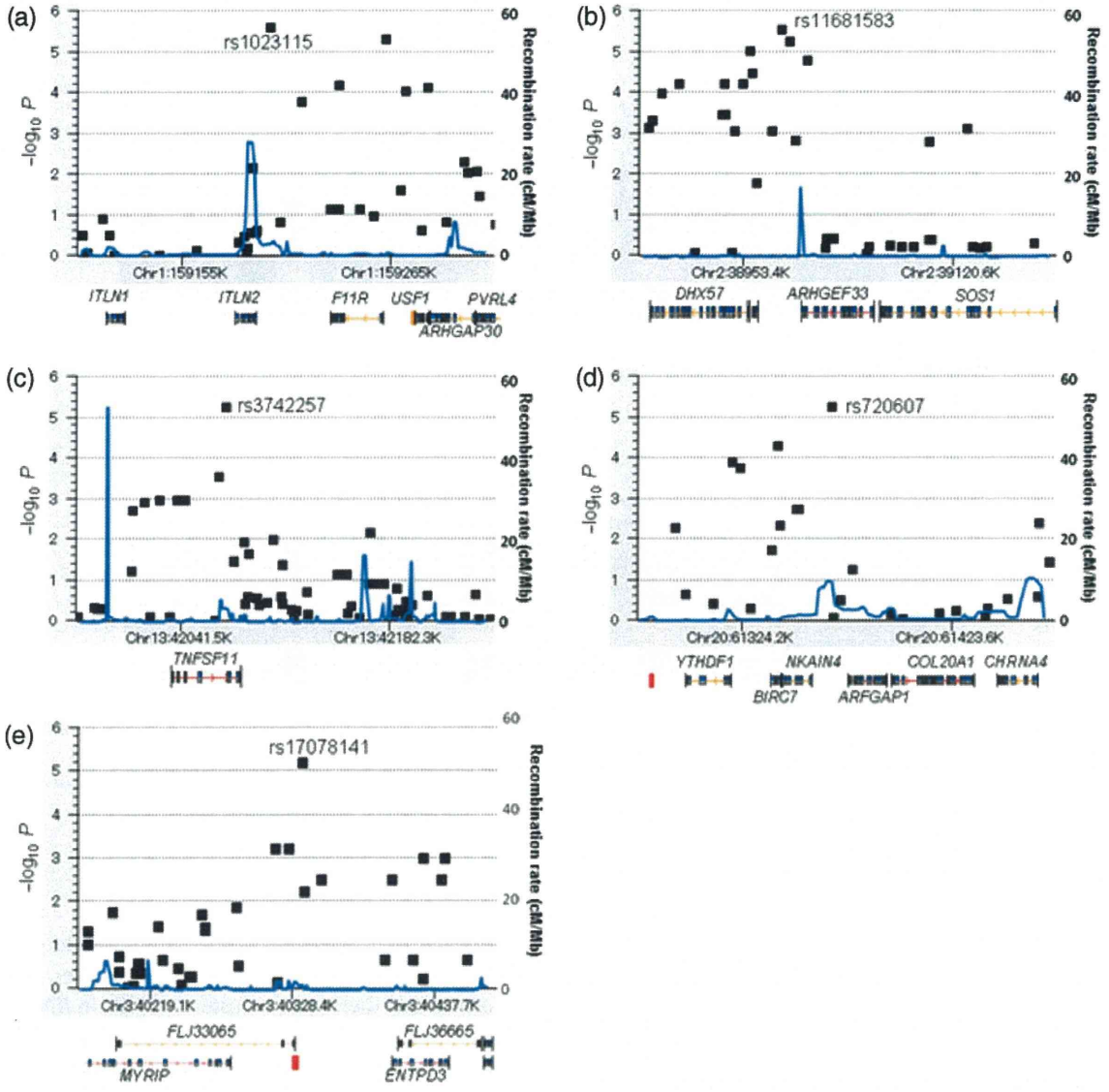

Figure 2. Regional association plots for the suggestive association regions. (a) Association plot for loci at rs1023115 on 1q23.3. (b) Association plot for loci at rs11681583 on 2p22.1. (c) Association plot for loci at rs720607 on 13q14.11. (d) Association plot for loci at rs2058364 on 20q13.33. (e) Association plot for loci at rs17078141 on 3p22.1. The results ($-\log_{10} P$) are for SNPs in the regions flanking the top SNPs. The recombination rate (blue line) was estimated based on the CEU, YRI and JPT+CHB populations from the Phase 2 HapMap (Release 22, NCBI 36). The annotated genes within the suggestive association regions are shown beneath the plots.

such predominant susceptible or causative rare variant in Caucasian cases as it is in East Asian MMD. Second, the rare variants cannot be discovered through GWAS. Next-generation sequencing will be of help in identifying rare variants. Third, several missense variants identified in candidate genes were unlikely to be causative genes because they are common in general Caucasian population. Searching for mutations by exome in a large number of Caucasian patients in these candidate genes is needed in future to find causative genes.

In summary, we were unsuccessful in our attempt to identify predominant founder variants in Caucasian MMD. The absence of the founder variant in Caucasians is in strong contrast to the major founder variant that has been identified in East Asians. Taken together, the present result probably indicates that locus heterogeneity as well as disease heterogeneity may be much greater in Caucasian MMD than in Asian MMD. Further study is warranted to investigate the genetic basis for global MMD.

Acknowledgements

This work was supported mainly by grants from the Ministry of Education, Culture, Sports, Science and Technology of Japan (Kiban Kenkyu A: 22249020) and the Ministry of Health, Labour and Welfare of Japan (H23-Nanji-Ippan-019, chaired by Dr Nobuo

Hashimoto) and partially by a grant from Creative Scientific Research (19G50314). We thank all individuals for their participation in this study. We also thank Dr David Školoudík (Department of Neurology, University Hospital, Ostrava, Czech Republic); Dr Martin Kucharík (Department of Neurology, 1st Faculty of Medicine, Charles University and General Teaching Hospital, Prague, Czech Republic); Dr Aleš Tomek (Department of Neurology, 2nd Faculty of Medicine, Charles University and Motol University Hospital, Prague, Czech Republic); Dr Martin Kovář (Department of Neurology, Na Homolce Hospital, Prague, Czech Republic); Dr Jan Fiksa (Department of Neurology, Military University Hospital, Prague, Czech Republic); Dr Michael J. Schmeisser (Institute for Anatomy and Cell Biology, Ulm University, Ulm, Germany); Dr Vera Alexandra Neves dos Santos (Department of Pediatry, Hospital de Faro, Faro, Portugal); Dr Vera Peters (Department of Neurosurgery, University of Tübingen, Tübingen, Germany); Prof. Daniela Berg and Ms Claudia Schulte (both Department of Neurology, University of Tübingen, Tübingen, Germany) and Prof. Martin Schöning (Department of Pediatrics, University of Tübingen, Tübingen, Germany) for their patients recruitment.

References

Fukuda M. and Kuroda T. S. 2002 Slac2-c (synaptotagmin-like protein homologue lacking C2 domains-c), a novel linker protein that interacts with Rab27, myosin Va/VIIa, and actin. *J. Biol. Chem.* **277**, 43096–43103.

Goto Y. and Yonekawa Y. 1992 Worldwide distribution of moyamoya disease. *Neurol. Med. Chir. (Tokyo)* **32**, 883–886.

Guo D. C., Papke C. L., Tran-Fadulu V., Regalado E. S., Avidan N., Johnson R. J. *et al.* 2009 Mutations in smooth muscle alpha-actin (ACTA2) cause coronary artery disease, stroke, and Moyamoya disease, along with thoracic aortic disease. *Am. J. Hum. Genet.* **84**, 617–627.

Kuroda S. and Houkin K. 2008 Moyamoya disease: current concepts and future perspectives. *Lancet Neurol.* **7**, 1056–1066.

Liu W., Hashikata H., Inoue K., Matsuura N., Mineharu Y., Kobayashi H. *et al.* 2010 A rare Asian founder polymorphism of Raptor may explain the high prevalence of Moyamoya disease among East Asians and its low prevalence among Caucasians. *Environ. Health Prev. Med.* **15**, 94–104.

Liu W., Morito D., Takashima S., Mineharu Y., Kobayashi H., Hitomi T. *et al.* 2011 Identification of RNF213 as a susceptibility gene for moyamoya disease and its possible role in vascular development. *PLoS One* **6**, e22542.

Liu W., Harada K. H., Hitomi T., Kobayashi H. and Koizumi A. 2012 Distribution of moyamoya disease susceptibility polymorphism p.R4810K in RNF213 in East and Southeast Asian populations. *Neurol. Med. Chir. (Tokyo)* **52**, 299–303.

Miyatake S., Miyake N., Touho H., Nishimura-Tadaki A., Kondo Y., Okada I. *et al.* 2012 Homozygous c.14576G>A variant of RNF213 predicts early-onset and severe form of moyamoya disease. *Neurology* **78**, 803–810.

Roder C., Peters V., Kasuya H., Nishizawa T., Wakita S., Berg D. *et al.* 2011 Analysis of ACTA2 in European Moyamoya disease patients. *Eur. J. Paediatr. Neurol.* **15**, 117–122.

Shimojima K. and Yamamoto T. 2009 ACTA2 is not a major disease-causing gene for moyamoya disease. *J. Hum. Genet.* **54**, 687–688.

Suzuki J. and Takaku A. 1969 Cerebrovascular "moyamoya" disease. Disease showing abnormal net-like vessels in base of brain. *Arch. Neurol.* **20**, 288–299.

Takeuchi K. and Shimizu K. 1957 Hypogenesis of bilateral internal carotid arteries. *Brain Nerve* **9**, 37–43.

Wu Z., Jiang H., Zhang L., Xu X., Zhang X., Kang Z. *et al.* 2012 Molecular analysis of RNF213 gene for moyamoya disease in the Chinese Han population. *PLoS One* **7**, e48179.

Received 16 February 2013, in revised form 15 June 2013; accepted 25 July 2013
Published on the Web: 10 December 2013

Biochemical and Biophysical Research Communications 439 (2013) 419–426

Contents lists available at ScienceDirect

Biochemical and Biophysical Research Communications

journal homepage: www.elsevier.com/locate/ybbrc

The moyamoya disease susceptibility variant RNF213 R4810K (rs112735431) induces genomic instability by mitotic abnormality

Toshiaki Hitomi [a,1], Toshiyuki Habu [b,1], Hatasu Kobayashi [a], Hiroko Okuda [a], Kouji H. Harada [a], Kenji Osafune [c], Daisuke Taura [d], Masakatsu Sone [d], Isao Asaka [c], Tomonaga Ameku [c], Akira Watanabe [c], Tomoko Kasahara [c], Tomomi Sudo [c], Fumihiko Shiota [c], Hirokuni Hashikata [e], Yasushi Takagi [e], Daisuke Morito [f], Susumu Miyamoto [e], Kazuwa Nakao [d], Akio Koizumi [a,*]

[a] Department of Health and Environmental Sciences, Graduate School of Medicine, Kyoto University, Kyoto, Japan
[b] Radiation Biology Center, Kyoto University, Kyoto, Japan
[c] Center for iPS Cell Research and Application (CiRA), Kyoto University, Kyoto, Japan
[d] Department of Medicine and Clinical Science, Graduate School of Medicine, Kyoto University, Kyoto, Japan
[e] Department of Neurosurgery, Graduate School of Medicine, Kyoto University, Kyoto, Japan
[f] Faculty of Life Sciences, Kyoto Sangyo University, Kyoto, Japan

ARTICLE INFO

Article history:
Received 16 August 2013
Available online 27 August 2013

Keywords:
Moyamoya disease
iPS cells
Mitotic phase
Genomic instability
Rs112735431
MAD2

ABSTRACT

Moyamoya disease (MMD) is a cerebrovascular disease characterized by occlusive lesions in the Circle of Willis. The RNF213 R4810K polymorphism increases susceptibility to MMD. In the present study, we characterized phenotypes caused by overexpression of RNF213 wild type and R4810K variant in the cell cycle to investigate the mechanism of proliferation inhibition. Overexpression of RNF213 R4810K in HeLa cells inhibited cell proliferation and extended the time of mitosis 4-fold. Ablation of spindle checkpoint by depletion of mitotic arrest deficiency 2 (MAD2) did not shorten the time of mitosis. Mitotic morphology in HeLa cells revealed that MAD2 colocalized with RNF213 R4810K. Immunoprecipitation revealed an RNF213/MAD2 complex: R4810K formed a complex with MAD2 more readily than RNF213 wild-type. Desynchronized localization of MAD2 was observed more frequently during mitosis in fibroblasts from patients ($n = 3$, $61.0 \pm 8.2\%$) compared with wild-type subjects ($n = 6$, $13.1 \pm 7.7\%$; $p < 0.01$). Aneuploidy was observed more frequently in fibroblasts ($p < 0.01$) and induced pluripotent stem cells (iPSCs) ($p < 0.03$) from patients than from wild-type subjects. Vascular endothelial cells differentiated from iPSCs (iPSECs) of patients and an unaffected carrier had a longer time from prometaphase to metaphase than those from controls ($p < 0.05$). iPSECs from the patients and unaffected carrier had significantly increased mitotic failure rates compared with controls ($p < 0.05$). Thus, RNF213 R4810K induced mitotic abnormalities and increased risk of genomic instability.

1. Introduction

Moyamoya disease (MMD: MIM 607151) is characterized by occlusive lesions at the terminal portion of internal carotid arteries in the Circle of Willis [1,2]. It is now recognized as one of the major causes of stroke in adults and children worldwide [3–6]. RNF213 has been recognized as the susceptibility gene for MMD, and the p. R4810K polymorphism (rs112735431 or ss179362673: G > A; herein referred to as RNF213 R4810K) as a founder variant commonly found in East Asian (Japanese, Korean and Chinese) MMD patients [7].

We recently found that vascular endothelial cells developed from induced pluripotent stem cells (iPSECs) of patients with MMD, carrying RNF213 R4810K, had reduced angiogenic activity [8]. This was partially mediated by the down-regulation of *Securin* [8]. In addition to *Securin*, various mitosis-associated genes were down regulated in iPSECs from patients [8]. Furthermore, the overexpression of RNF213 R4810K inhibited the proliferation of human umbilical vein endothelial cells (HUVECs) [8]. The primary aim of our study was to characterize the phenotypes associated with RNF213 R4810K in the cell cycle.

* Corresponding author. Address: Department of Health and Environmental Sciences, Graduate School of Medicine, Kyoto University, Konoe-cho, Yoshida, Sakyo-ku, Kyoto 606-8501, Japan. Fax: +81 75 753 4458.
E-mail address: koizumi.akio.5v@kyoto-u.ac.jp (A. Koizumi).
[1] These authors contributed equally to this work.

0006-291X/$ - see front matter © 2013 Elsevier Inc. All rights reserved.
http://dx.doi.org/10.1016/j.bbrc.2013.08.067

2. Methods

2.1. Participants

We studied three probands from three unrelated families with MMD, a carrier of RNF213 R4810K and seven controls. Details of the patients were described previously [8] and in Table S1. We obtained written informed consent from all participants in this study. Our study was approved by the Institutional Ethical Review Board of Kyoto University.

2.2. Cell culture and transfection

Fibroblasts and HeLa cells were maintained in Dulbecco's Minimal Essential Medium (DMEM; Invitrogen, Tokyo, Japan) containing 10% fetal bovine serum (FBS; Japan Bioserum, Hiroshima, Japan). Fibroblasts from passages 3–5 were used for all experiments. Induced pluripotent stem cells (iPSCs) were maintained as previously reported [8,9].

An mCherry-tagged wild-type RNF213 or an mCherry-tagged RNF213 R4810 K was cloned into pcDNA3.1 (Invitrogen) (Fig. S1) [8]. To monitor the localization of MAD2, HeLa cells stably expressing EGFP-MAD2 were used. MAD2 cDNA cloned into pEGFP-C1 (Clontech Laboratories, Palo Alto, CA, USA) was introduced into HeLa cells, and a G418-resistant clone was verified by western blotting and fluorescent microscopy. The plasmid was introduced into HeLa cells using Lipofectamine 2000 (Invitrogen) and successfully transfected cells selected with 500 μg/ml G418 (Nacalai Tesque, Kyoto, Japan) for 10 days.

Transfection of small interfering RNAs (siRNAs) was conducted using Dharmafect (#1 or #3; Dharmacon, Lafayette, CO, USA) as previously reported [8]. We purchased and used RNF213 siRNA (Santa Cruz Biotechnology) and MAD2 siRNA (Santa Cruz Biotechnology) with control siRNA-A (Santa Cruz Biotechnology) used as controls.

2.3. Karyotyping

For karyotyping, fibroblasts from six controls (Control 1 to Control 6), one carrier, and three patients were treated with nocodazole (100 ng/ml) for 72 h. Well-isolated chromosomes were chosen and counted three times for each chromosome set. For each fibroblast culture, duplicate karyotyping experiments were conducted. For MAD2 staining, fibroblasts were treated with nocodazole (100 ng/ml) for 72 h, fixed with 4% paraformaldehyde and permeabilized in phosphate-buffered saline (PBS) containing 0.2% Triton X-100. An anti-MAD2 antibody (Covance, Berkeley, CA, USA) was used for immunostaining.

To evaluate chromosomal instability, six iPSC clones from controls (Control 1 to Control 7 except Control 4) and four from a carrier and patients were karyotyped (Table S1).

2.4. Colony formation assays

Following transfection, HeLa cells were reseeded at densities of 1×10^3 to 2.7×10^4 cells/100-mm dish and maintained in DMEM with 10% FBS for 5 days. Medium containing G418 (Nacalai Tesque) was exchanged twice a week. After 10 days, resistant colonies were scored using formalin fixation and crystal violet staining.

2.5. Time-lapse imaging using confocal laser scanning microscopy

Transfected HeLa cells and iPSECs were plated on 35-mm glass-bottom culture dishes. Time-lapse 3D imaging was performed using an FV10i confocal microscope (Olympus, Tokyo, Japan) at 37 °C/5% CO_2. The recording interval was 40 min, and Z-stack images were generated with Fluoview (Olympus).

2.6. Western blotting

Samples were subjected to immunoblotting using the anti-RNF213 antibody, which we generated previously [8], anti-MAD2, anti-dsRed (BD Biosciences), or anti-β-actin (Abcam, Cambridge, UK) antibodies. Quantitation was conducted using Image J software.

2.7. Co-immunoprecipitation of MAD2 with RNF213

HeLa cells transiently expressing the wild-type RNF213 mCherry or RNF213 R4810K mCherry or naïve HeLa cells were lysed in RIPA buffer without sodium dodecyl sulfate (SDS) but with protease inhibitors (Nacalai Tesque). Cell lysates from 4×10^6 cells were incubated with protein A agarose (Santa Cruz Biotechnology) for 30 min at 4 °C with normal mouse immunoglobulin G (IgG; MBL, Nagoya, Japan). After magnetic separation, beads were discarded and supernatants incubated for 4 h at 4 °C with a monoclonal anti-dsRed or polyclonal anti-RNF213 antibody [8] followed by magnetic beads for 4 h. Beads were washed three times with lysis buffer, and bound proteins dissolved in SDS sample buffer at 95 °C for 5 min, subjected to SDS polyacrylamide gel electrophoresis (PAGE) and analyzed by western blotting with anti-MAD2 antibody.

2.8. Statistical analysis

Results are presented as the mean ± standard deviation (SD) unless otherwise stated. Differences between groups were analyzed using analysis of variance (ANOVA), followed by Tukey's honestly significant difference test for comparisons involving more than two means (SAS Institute Inc., Cary, NC, USA). The variance in chromosome numbers as determined by karyotyping was compared with controls using an F-test. Subcellular localization of MAD2 was categorized into four groups and compared with controls using Fisher's exact test with Bonferroni correction. A p-value with Bonferroni correction less than 0.05 was considered statistically significant.

3. Results

3.1. Effects of RNF213 R4810K overexpression

mCherry-tagged wild-type RNF213 and/or RNF213 R4810K proteins (Fig. S1) were overexpressed in HeLa cells (Fig. S2A and B). Localization of exogenous RNF213 R4810K was similar to that of exogenous and endogenous wild-type RNF213, where proteins were observed in the cytoplasm around the nucleus (Fig. S2B). Overexpression of RNF213 R4810K highly repressed colony formation units of HeLa cells (Fig. S2C). In contrast, RNAi-mediated depletion of RNF213 in HeLa cells did not repress colony formation units (Fig. S2D).

To understand better the causes underlying inhibition of cell proliferation, cell cycle distribution of HeLa cells expressing wild-type RNF213 and RNF213 R4810K were monitored. Overexpression of RNF213 R4810K caused a G2/M-plus-higher-DNA-content (4N>) accumulation in HeLa cells (Fig. S3), but overexpression of wild-type of RNF213 did not. Live imaging analyses showed that mitotic stages were severely delayed in HeLa cells overexpressing RNF213 R4810K (Fig. 1A–C). In cells overexpressing the control vector, wild-type RNF213, control siRNA or RNF213 siRNA, the mean time from prometaphase to metaphase was 37 ± 10 min: The mean time

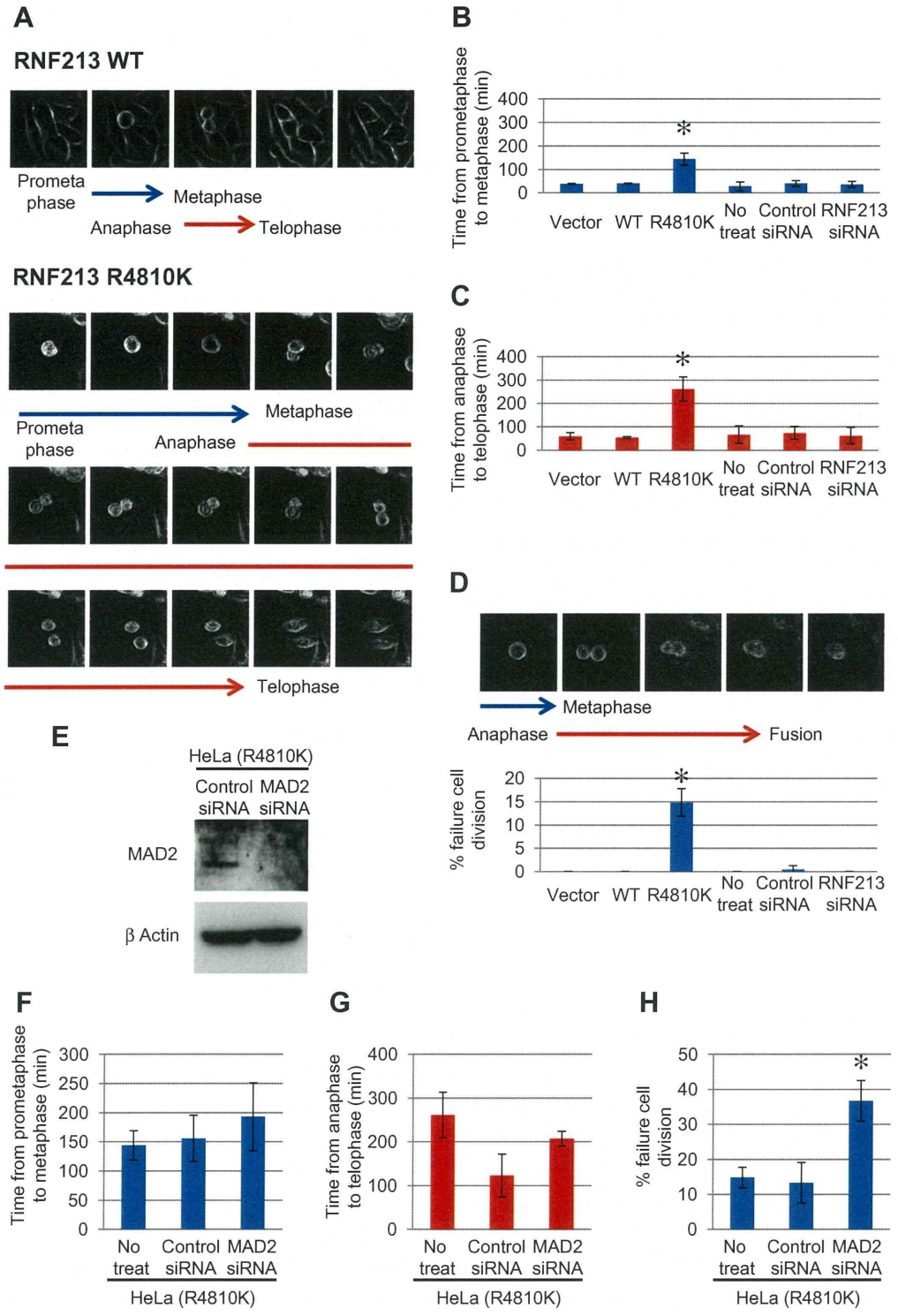

Fig. 1. Time-lapse imaging of HeLa cells transfected with wild-type RNF213 and RNF213 R4810K, or control siRNA, RNF213 siRNA and MAD2 siRNA. (A) Representative time-lapse images showing wild-type RNF213 and RNF213 R4810K. Images were obtained every 40 min. (E) Western blot analysis of HeLa cells overexpressing RNF213 R4810K with MAD2 siRNA transfection. (B, C, F, G) The period of time from prometaphase to metaphase, and from anaphase to telophase. A total of 20 cells were observed in three areas for each group. (D, H) Failed cell division in HeLa cells overexpressing RNF213 R4810K transfected with control siRNA and MAD2 siRNA. Cells ($n = 40$) were counted in three areas for each group. Values are presented as means ± SDs. $^*p < 0.05$.

from anaphase to telophase was 63 ± 24 min (Fig. 1B and C). In contrast, for cells overexpressing RNF213 R4810K, progression from prometaphase to metaphase was 144 ± 25 min, while the progression from anaphase to telophase was 261 ± 52 min (Fig. 1B and C). Overexpression of RNF213 R4810K resulted in several daughter cells that failed to complete cell division. For 14.8 ± 2.9% of the total cell population, cytokinesis failed to occur (Fig. 1D).

We investigated whether activation of spindle checkpoint was responsible for the delayed mitotic progression phenotype in HeLa cells overexpressing RNF213 R4810K. We inhibited spindle checkpoint by depletion of MAD2, which senses mitotic progression, and

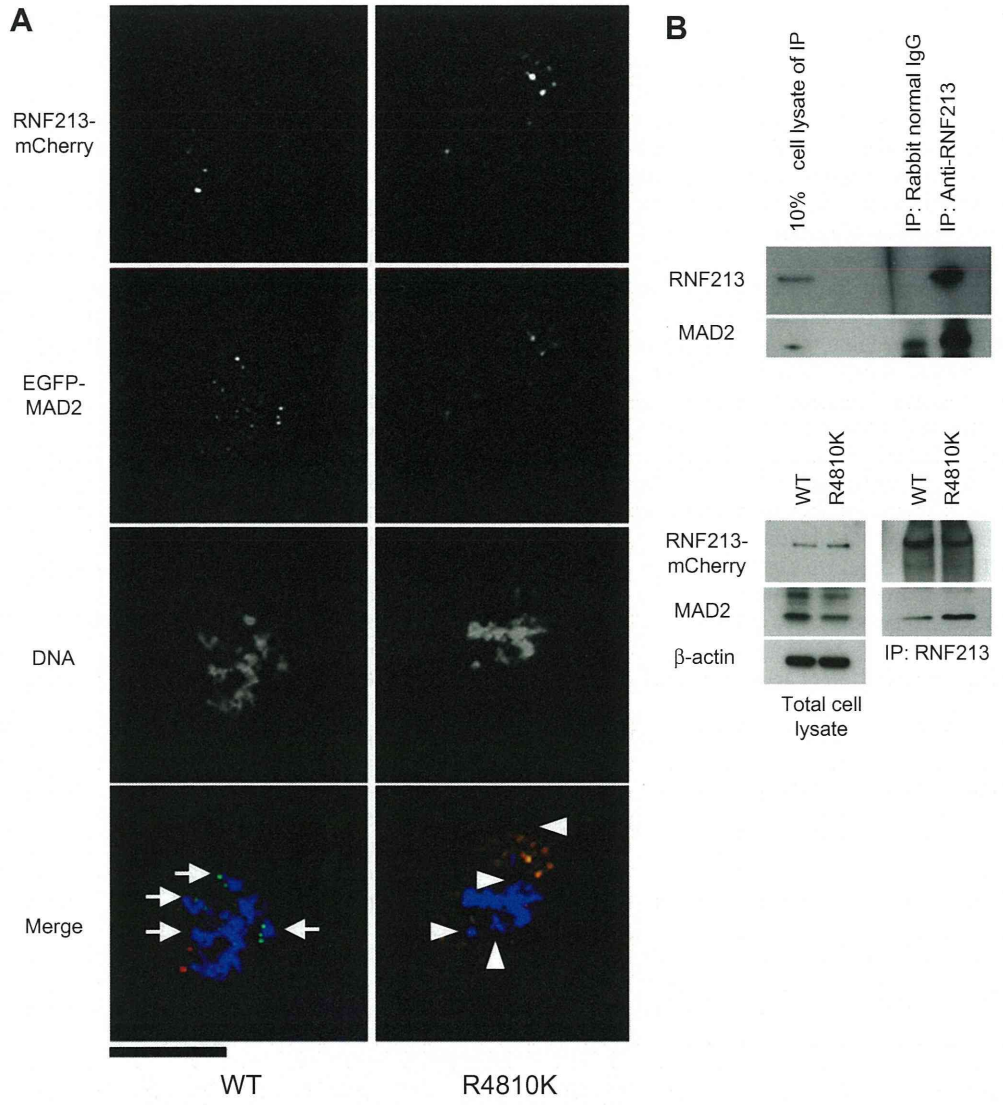

Fig. 2. Colocalization of RNF213 R4810K with MAD2 at prometaphase. (A) MAD2 localization in HeLa cells overexpressing wild-type RNF213 and RNF213 R4810K. Wild-type RNF213-mCherry (left panels; WT) or RNF213 R4810K-mCherry (right panels; R4810K) plasmids were introduced into HeLa cells stably expressing EGFP-MAD2. Red, green and blue staining corresponded to signals for RNF213-mCherry, EGFP-MAD2 and DNA, respectively. MAD2-positive lagging chromosomes in cells overexpressing wild-type RNF213 are indicated by arrows. Lagging chromosomes without MAD2 signals in cells overexpressing RNF213 R4810K are indicated by arrowheads. The scale bar indicates 20 μm. (B) Upper panel: HeLa cells were lysed and subjected to immunoprecipitation (IP) using rabbit normal IgG or an anti-RNF213 antibody. Ten-fold diluted cell lysate and the immunoprecipitated samples were immunoblotted using anti-RNF213 and anti-MAD2 antibodies. Lower panel: HeLa cells transiently expressing wild-type RNF213-mCherry (WT) or RNF213 R4810K-mCherry (R4810K) were lysed and subjected to IP using an anti-dsRed antibody. Total cell lysate and the IP samples were immunoblotted using anti-dsRed and anti-MAD2 antibodies. β-Actin was used as a loading control. (For interpretation of the references to color in this figure legend, the reader is referred to the web version of this article.)

conducted live image analysis (Fig. 1E–G). Depletion of MAD2 did not shorten the time in mitosis. In contrast, the mitotic failure rate was further increased by depletion of MAD2 in HeLa cells overexpressing RNF213 R4810K (Fig. 1H).

The localization of RNF213 was also analyzed during the mitotic phase by tracking MAD2 localization. In cells transfected with wild-type RNF213, MAD2 was localized onto the kinetochore during prometaphase, and translocated to centrosomes with RNF213 during the metaphase to anaphase transition (Figs. 2A and S4) as reported [10,11]. Signals corresponding to mCherry-tagged wild-type RNF213 were colocalized with MAD2 on mitotic microtubules around centrosomes during metaphase (Fig. S4). In contrast, we observed abnormal localization of MAD2 in cells overexpressing RNF213 R4810K. During prometaphase, MAD2 signals were not observed onto kinetochores but colocalized with RNF213 R4810K on mitotic microtubules around centrosomes (Fig. 2A). Localization of signals corresponding to mCherry-tagged RNF213 R4810K was, however, similar to that in cells overexpressing wild-type RNF213 during metaphase (Fig. S4).

The colocalization of MAD2 and RNF213 R4810K led us to investigate whether RNF213 R4810K or wild-type RNF213 could form a complex with MAD2. Both endogenous and exogenous wild-type RNF213 were co-immunoprecipitated by an anti-RNF213 antibody with endogenous MAD2 from HeLa cell extracts (Fig. 2B). A greater quantity of MAD2 was co-immunoprecipitated with the complex containing RNF213 R4810K compared with that containing wild-type RNF213. These data collectively suggest that the effects of MAD2 depletion on mitotic failure phenotype can override the mislocalization of MAD2 induced by overexpression of RNF213 R4810K in an additive manner while the effect on delayed mitotic progression phenotype is saturated.

3.2. iPSC karyotypes and mitotic abnormality in human fibroblasts

iPSCs from six fibroblast clones had normal karyotypes, but those from three MMD patients had abnormal karyotypes (Table S1, Fig. S5). The incidence of abnormal karyotypes in iPSC clones from subjects with RNF213 R4810K was 75% (3/4), while none of the six iPSC clones with wild-type RNF213 (0/6) had abnormal karyotypes (Fisher's exact test, $p < 0.03$). We then examined mitotic defects in primary fibroblasts from controls, the unaffected carrier and MMD patients (Table S1). All fibroblasts had normal karyotypes. We also searched for potential mitotic defects that may have been inherent in primary fibroblasts in patients with MMD by activating the spindle checkpoint with nocodazole. MAD2 signals and mitotic morphology were observed 72 h after treatment with nocodazole. Treatment with nocodazole depolymerizes microtubules and attached microtubules are detracted from kinetochores. Therefore, MAD2 should have been mobilized onto unattached kinetochores. In fact, in control cells, the majority of MAD2 was observed at the kinetochores. However, large quantities of MAD2 did not bind to the kinetochores of lagging chromosomes (Fig. 3) in fibroblasts from patients with RNF213 R4810K ($n = 3$, $61.0 \pm 8.2\%$) compared with those from controls ($n = 6$, $13.1 \pm 7.7\%$; $p < 0.01$). Furthermore, aneuploidy was observed more frequently in fibroblasts from MMD patients than in controls (Fig. 4A). Even under the condition of activated spindle checkpoint by nocodazole, distances of sister chromatids were widened in patient 1 and patient 2 and sister chromatids were separated completely in patient 3 (Fig. 4B). Premature sister chromatid separation can induce karyotype abnormality. Taken together these observations, the mislocalization of MAD2, aneuploidy and premature sister chromatid separation, consistently suggest mitotic abnormalities.

Next live image analyses for iPSECs from patients, Patient 1(GA), 2 (AA) and 3 (AA), an unaffected carrier (GA) and controls, Control 1 and 2 (GG) were conducted (Fig. 4C). The mean time (min) from prometaphase to metaphase was significantly longer (GA; 79.2 ± 72.1 or AA; 94.4 ± 86.3) for iPSECs from patients and unaffected carrier than from controls (42.0 ± 30.3; $p < 0.05$). However, the mean time from metaphase to anaphase for iPSECs from patients and unaffected carrier was not different from that for iPSECs from controls ($p > 0.05$). It is interesting that the mitotic failure rate (%) was also significantly higher for iPSECs from the patients and unaffected carrier (GA; 13.0 ± 3.2 or AA; 21.2 ± 4.0) than from the controls (1.9 ± 3.2; $p < 0.05$). The phenomena observed in HeLa cells overexpressing RNF213 R4810K were recaptured in iPSECs heterozygous and homozygous for RNF213 R4810K, suggesting that mitotic abnormality is genuinely associated with RNF213 R4810K.

4. Discussion

In this study, we demonstrated that RNF213 R4810K adversely affected the localization of MAD2 to the kinetochore during mitosis. Furthermore, RNF213 colocalized with MAD2 by confocal microscopy and immunoprecipitation confirmed both endogenous and exogenous wild-type RNF213 and RNF213 R4810K formed complexes with MAD2. The MAD2 complex with RNF213 R4810K captured a greater quantity of MAD2 than the complex with wild-type RNF213, suggesting a larger capturing capacity. The abnormal localization of MAD2 and mitotic abnormality were confirmed in primary fibroblasts from MMD patients. Furthermore, we observed more frequent karyotype abnormality in iPSCs from MMD patients compared with wild-type controls.

These findings indicate that RNF213 R4810K induces phenotypes associated with mitotic abnormalities. It is well known that genetic defects in cell cycle-related proteins are associated with steno-occlusive lesions around the Circle of Willis. These include Ras-MAPK pathway-related diseases (neurofibromatosis 1, Noonan syndrome, Castelo syndrome, Cranio-facio-cutaneous syndrome, and Alagille syndrome [12–14]) and cell cycle-related diseases (microcephalic osteodysplastic primordial dwarfism type II, Seckel syndrome and X-related moyamoya syndrome) [15]. The majority of cell cycle-related diseases are often accompanied by somatic undergrowth. It is likely that cell cycle defects elevate the risk of cell death or mitotic failure due to defective mitosis and chromosomal missegregation, which may be a common inherent risk factor among diseases associated with moyamoya syndrome and MMD. This would adversely affect multiple organs, including the vascular system. In contrast, MMD is not complicated by somatic undergrowth. We speculate that mitotic defects in RNF213 R4810K carriers specifically emerge in vascular endothelial cells.

The current study demonstrated an elevated mitotic failure rate in iPSECs from MMD patients. When ECs are damaged, they may be peeled off from the vascular bed and then denudated vascular areas emerge. Such vascular denudation should be recovered by migration and proliferation of circulating endothelial progenitor cells. Unless otherwise, migration and proliferation of vascular smooth muscle cells (VSMCs) occur subsequently, resulting in intimal hyperplasia. It may be considered a limitation of our work that we did not investigate VSMCs. However, given the pathological model of the vascular injury induced by radiation [16], which is known to cause steno-occlusive lesion in intracranial artery [3], an initial pathological process in MMD may be reasonably assumed to be mediated by mitotic failure of endothelial cells (ECs) followed by the excessive proliferation of VSMCs. The interactions between ECs and VSMCs play key roles in maintaining vascular structure and the function of vessels [16]. VSMC migration, proliferation, and differentiation are critical processes involved in intimal hyperplasia and are regulated by ECs [16]. Thus, mitotic failure may impair the crosstalk between ECs and VSMCs in patients with MMD. Further studies focusing on cell cycle defects in VSMCs and the crosstalk between VSMCs and endothelial cells are necessary.

In the current study, delayed mitotic progression phenotypes of HeLa cells overexpressing RNF213 R4810K or of iPSECs from patients was consistently observed. To investigate whether spindle checkpoint activation is responsible for the delayed mitotic progression phenotype, the MAD2 signaling pathway was inhibited. Depletion of MAD2 did not shorten time in mitosis or induce mitotic exit in cells overexpressing RNF213 R4810K, indicating that spindle checkpoint may be inactivated in those cells. Depletion of MAD2, however, could override the mitotic failure phenotype of HeLa cells overexpressing RNF213 R4810K in an additive manner. These observations suggest overexpression of RNF213 R4810K causes MAD2 mislocalization and leads to inactivation of MAD2 function, which is further impaired by depletion of MAD2 in the phenotype of the mitotic failure. Previously, we reported that RNF213 R4810K suppressed gene expression of *Securin*, *SKA3*, *SGO1*, *CDC20* and *BUB1*[8]. It should be noted that depletion of *SKA3* and *SGO1* cause mitotic delays and premature sister chromatid separation [17]. Taken together, for mechanisms of mitotic abnormalities, a simple and straightforward explanation would be to assume that because *Securin* has dual mechanisms of separase regulation [18] and depletion of *Securin* slowed mitotic progression [19], RNF213 R4810K slowed mitotic progression by down-regulation of *Securin* and caused mitotic abnormalities by MAD2 mislocalization [20]. However, we cannot ignore other possibilities because other down regulated genes may cause mitotic abnormalities in a synergistic manner or an antagonistic manner. The most substantial event in mitotic abnormalities, however, is likely associated with the down regulation of a group of mitosis

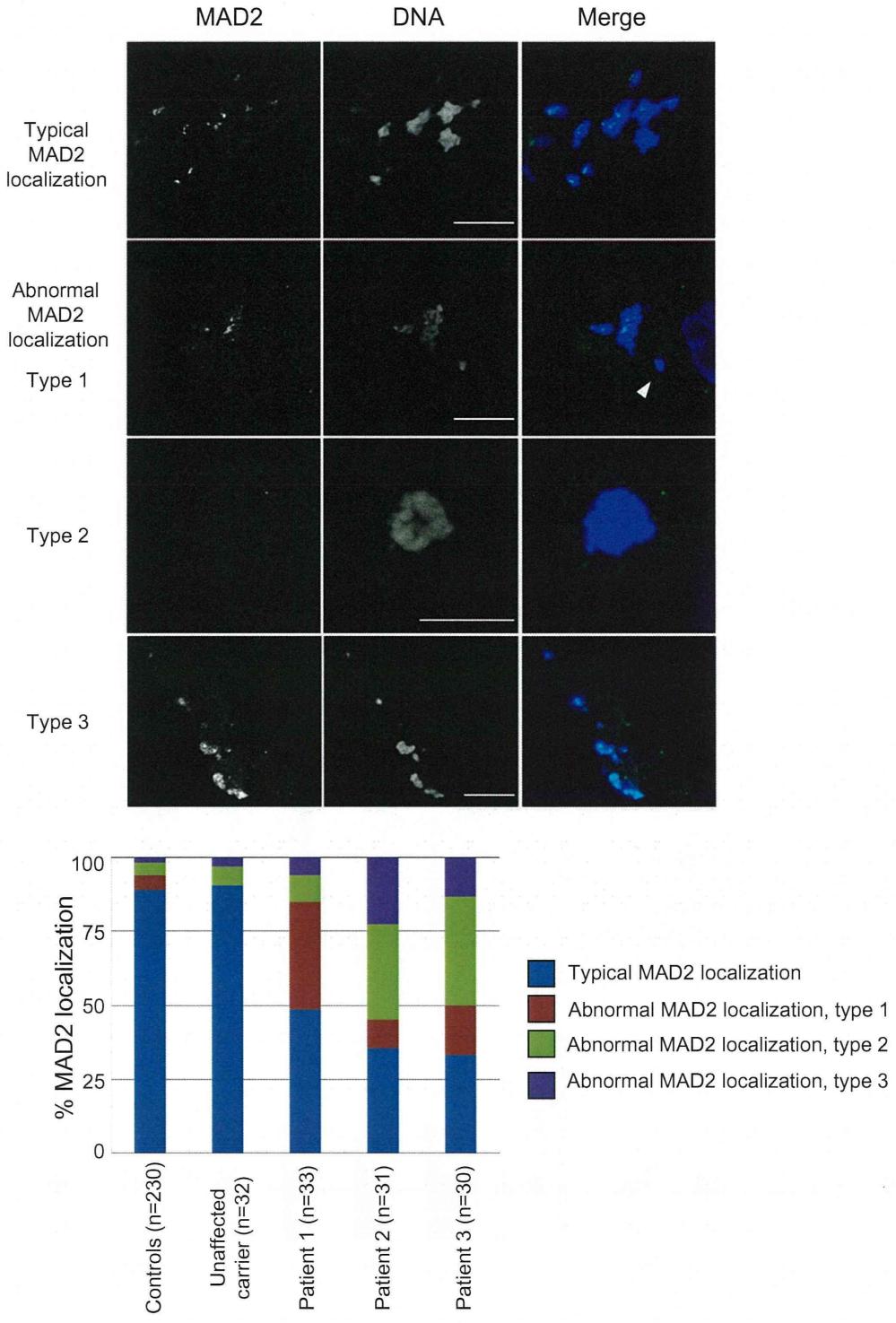

Fig. 3. Subcellular localization of MAD2 in fibroblasts from MMD patients at prometaphase. Fibroblasts from MMD patients ($n = 3$), an unaffected carrier ($n = 1$), or controls ($n = 6$) treated with nocodazole for 72 h were incubated with an antibody against MAD2. The numbers of examined chromosomes are shown in parentheses. For each subject, more than 30 chromosomes were investigated. Typical MAD2 signals (green) and nuclei (blue) in MMD fibroblasts are shown in the top panels. The scale bar represents 10 μm. Abnormal MAD2 staining patterns are shown in the lower panel. Abnormal MAD2 localization type 1 refers to MAD2-positive cells with MAD2-negative lagging chromosomes (arrowhead). Abnormal MAD2 localization type 2 refers to MAD2-negative cells. Abnormal MAD2 localization type 3 was defined as a distribution pattern of MAD2 that was not spotty, yet the protein was present and spread across the entire chromosome. The frequencies of the different MAD2 staining patterns in MMD fibroblasts were compared with controls using Fisher's exact test followed by Bonferroni correction. $p = 1.00$, unaffected carrier vs. controls; $p = 3.19 \times 10^{-11}$, patient 1 vs controls; $p = 8.77 \times 10^{-7}$, patient 2 vs controls; $p = 5.54 \times 10^{-10}$, patient 3 vs controls. (For interpretation of the references to color in this figure legend, the reader is referred to the web version of this article.)

associated genes by RNF213 R4810K. Further studies are needed to understand the mechanisms of RNF213 R4810K-induced down regulation of mitosis-associated genes and subsequent signaling deviations that induce mitotic abnormalities.

We observed an inhibition of cellular proliferation *in vitro*, but not in *ex vivo* studies [8]. We attributed these differences to acute and chronic effects. Acutely, there is very little adaptation to RNF213 R4810K overexpression; however, in chronic cases the cells

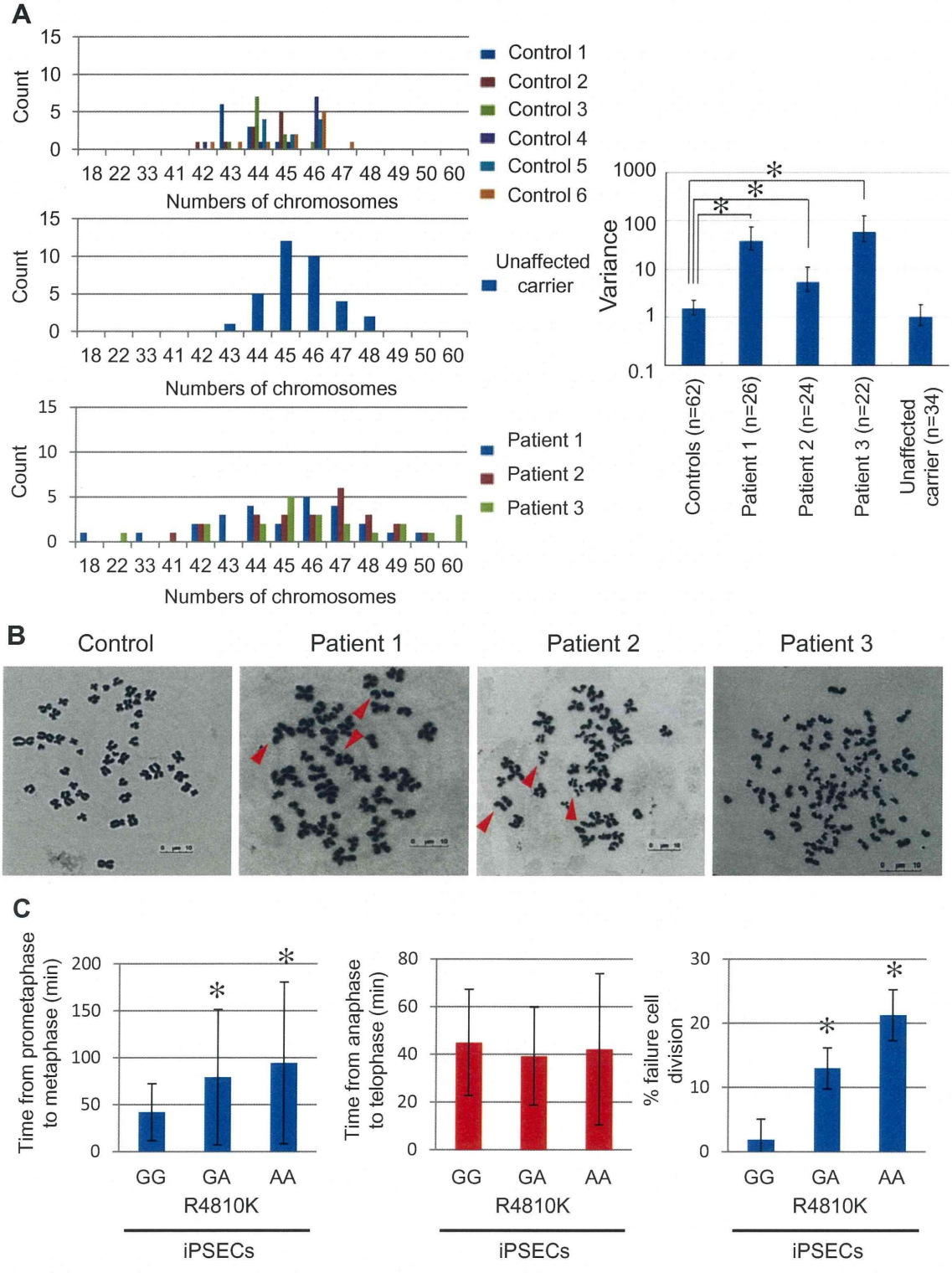

Fig. 4. Mitotic abnormality in fibroblasts and time-lapse imaging of iPSECs from MMD patients. (A) Karyotypes of MMD fibroblasts. Fibroblasts from MMD patients, the unaffected carrier or controls treated with nocodazole for 72 h were subjected to Giemsa staining. Fibroblasts from the controls (upper), carriers (middle), and MMD patients (lower) can be clearly seen. The variance in chromosome number is presented with a 95% confidence interval (right panel). Heterogeneity in the variance was tested using the *F*-test with Bonferroni correction for equality of variance. $^*p < 0.001$ using the *F*-test. (B) Typical morphologies of chromosomes stained with Giemsa in fibroblasts from MMD patients and controls. Prematurely separated chromosomes in the fibroblasts from patients 1 and 2 are indicated by arrowheads. Completely separated chromosomes in the fibroblasts from patient 3 are shown in the right panel. The typical morphology of fibroblasts from controls is presented in the left panel. The scale bar indicates 10 μm. (C) Time-lapse imaging of iPSECs from MMD patients and an unaffected carrier (GA or AA genotype) and controls (GG genotype). The period of time from prometaphase to metaphase, and from anaphase to telophase, and failed cell division were evaluated. Values are presented as means ± SDs. $^*p < 0.05$.

may adapt for the gain of function effects of this protein and mask the proliferative defects. Such discrepancies are often observed between acute and chronic effects [21–23].

In conclusion, this study demonstrated the sequestration of MAD2 by RNF213 R4810K during mitosis. The resultant defects including mitotic abnormalities were considered to increase genomic instability and thus be risk factors for MMD.

Funding sources

This work was supported by grants from the Ministry of Education, Culture, Sports, Science and Technology of Japan (Nos. 17109007 and 22249020 to Dr. Koizumi). This research was partially supported by the Japan Society for the Promotion of Science through its Funding Program for World-Leading Innovative R&D on Science and Technology (FIRST Program to Dr. Osafune).

Acknowledgments

We are grateful to Drs. Wanyang Liu, Shanika Nanayakkara, STMLD Senevirathna (Kyoto University Graduate School of Medicine) and Sasatani (Toyoshima) M (Hiroshima University) for their discussion.

Appendix A. Supplementary data

Supplementary data associated with this article can be found, in the online version, at http://dx.doi.org/10.1016/j.bbrc.2013.08.067.

References

[1] J. Suzuki, A. Takaku, Cerebrovascular "moyamoya" disease. Disease showing abnormal net-like vessels in base of brain, Arch. Neurol. 20 (1969) 288–299.
[2] K. Takeuchi, K. Shimizu, Hypogenesis of bilateral internal carotid arteries, Brain Nerv. 9 (1957) 37–43.
[3] S. Kuroda, K. Houkin, Moyamoya disease: current concepts and future perspectives, Lancet Neurol. 7 (2008) 1056–1066.
[4] W. Miao, P.L. Zhao, Y.S. Zhang, H.Y. Liu, Y. Chang, J. Ma, Q.J. Huang, Z.X. Lou, Epidemiological and clinical features of Moyamoya disease in Nanjing, China, Clin. Neurol. Neurosurg. 112 (2010) 199–203.
[5] R.M. Scott, E.R. Smith, Moyamoya disease and moyamoya syndrome, N. Engl. J. Med. 360 (2009) 1226–1237.
[6] A. Veeravagu, R. Guzman, C.G. Patil, L.C. Hou, M. Lee, G.K. Steinberg, Moyamoya disease in pediatric patients: outcomes of neurosurgical interventions, Neurosurg. Focus 24 (2008) E16.
[7] W. Liu, D. Morito, S. Takashima, Y. Mineharu, H. Kobayashi, T. Hitomi, H. Hashikata, N. Matsuura, S. Yamazaki, A. Toyoda, K. Kikuta, Y. Takagi, K.H. Harada, A. Fujiyama, R. Herzig, B. Krischek, L. Zou, J.E. Kim, M. Kitakaze, S. Miyamoto, K. Nagata, N. Hashimoto, A. Koizumi, Identification of RNF213 as a susceptibility gene for moyamoya disease and its possible role in vascular development, PLoS ONE 6 (2011) e22542.
[8] T. Hitomi, Habu, T., Kobayashi, H., Okuda, H., Harada, HK, Osafune, K., Taura, D., Sone, M., Adaka, I., Ameku, T., Watanabe, A., Kasahara, T., Sudo, T., Shiota, F., Hashikata, H., Takagi, Y., Morito, D., Miyamoto, S., Nakao K., and Koizumi, A., Down-regulation of Securin by the variant RNF213 R4810K may likely reduce angiogenic activity of induced pluripotent stem cells- derived vascular endothelial cells from moyamoya patients, Biochem. Biophys. Res. Commun. **438**, (2013), 13-19.
[9] K. Takahashi, K. Tanabe, M. Ohnuki, M. Narita, T. Ichisaka, K. Tomoda, S. Yamanaka, Induction of pluripotent stem cells from adult human fibroblasts by defined factors, Cell 131 (2007) 861–872.
[10] B.J. Howell, D.B. Hoffman, G. Fang, A.W. Murray, E.D. Salmon, Visualization of Mad2 dynamics at kinetochores, along spindle fibers, and at spindle poles in living cells, J. Cell Biol. 150 (2000) 1233–1250.
[11] Y. Li, R. Benezra, Identification of a human mitotic checkpoint gene: hsMAD2, Science 274 (1996) 246–248.
[12] W.E. Tidyman, K.A. Rauen, Noonan, Costello and cardio-facio-cutaneous syndromes: dysregulation of the Ras-MAPK pathway, Exp. Rev. Mol. Med. 10 (2008) e37.
[13] B.M. Kamath, N.B. Spinner, K.M. Emerick, A.E. Chudley, C. Booth, D.A. Piccoli, I.D. Krantz, Vascular anomalies in Alagille syndrome: a significant cause of morbidity and mortality, Circulation 109 (2004) 1354–1358.
[14] M. Noseda, L. Chang, G. McLean, J.E. Grim, B.E. Clurman, L.L. Smith, A. Karsan, Notch activation induces endothelial cell cycle arrest and participates in contact inhibition: role of p21Cip1 repression, Mol. Cell. Biol. 24 (2004) 8813–8822.
[15] A. Koizumi, H. Kobayashi, T. Hitomi, Genes associated with moyamoya syndrome and disease, No Shinkei Geka 40 (2012) 105–118.
[16] F. Milliat, A. Francois, M. Isoir, E. Deutsch, R. Tamarat, G. Tarlet, A. Atfi, P. Validire, J. Bourhis, J.C. Sabourin, M. Benderitter, Influence of endothelial cells on vascular smooth muscle cells phenotype after irradiation: implication in radiation-induced vascular damages, Am. J. Pathol. 169 (2006) 1484–1495.
[17] J.R. Daum, J.D. Wren, J.J. Daniel, S. Sivakumar, J.N. McAvoy, T.A. Potapova, G.J. Gorbsky, Ska3 is required for spindle checkpoint silencing and the maintenance of chromosome cohesion in mitosis, Curr. Biol. 19 (2009) 1467–1472.
[18] N.C. Hornig, P.P. Knowles, N.Q. McDonald, F. Uhlmann, The dual mechanism of separase regulation by securin, Curr. Biol. 12 (2002) 973–982.
[19] L.J. Holt, A.N. Krutchinsky, D.O. Morgan, Positive feedback sharpens the anaphase switch, Nature 454 (2008) 353–357.
[20] L. Michel, E. Diaz-Rodriguez, G. Narayan, E. Hernando, V.V. Murty, R. Benezra, Complete loss of the tumor suppressor MAD2 causes premature cyclin B degradation and mitotic failure in human somatic cells, Proc. Natl. Acad. Sci. USA 101 (2004) 4459–4464.
[21] F. Iovino, L. Lentini, A. Amato, A. Di Leonardo, RB acute loss induces centrosome amplification and aneuploidy in murine primary fibroblasts, Mol. Cancer 5 (2006) 38.
[22] J. Mei, X. Huang, P. Zhang, Securin is not required for cellular viability, but is required for normal growth of mouse embryonic fibroblasts, Curr. Biol. 11 (2001) 1197–1201.
[23] K. Pfleghaar, S. Heubes, J. Cox, O. Stemmann, M.R. Speicher, Securin is not required for chromosomal stability in human cells, PLoS Biol. 3 (2005) e416.

Biochemical and Biophysical Research Communications 438 (2013) 13–19

Contents lists available at SciVerse ScienceDirect

Biochemical and Biophysical Research Communications

journal homepage: www.elsevier.com/locate/ybbrc

Downregulation of Securin by the variant RNF213 R4810K (rs112735431, G>A) reduces angiogenic activity of induced pluripotent stem cell-derived vascular endothelial cells from moyamoya patients

Toshiaki Hitomi [a,1], Toshiyuki Habu [b,1], Hatasu Kobayashi [a], Hiroko Okuda [a], Kouji H. Harada [a], Kenji Osafune [c], Daisuke Taura [d], Masakatsu Sone [d], Isao Asaka [c], Tomonaga Ameku [c], Akira Watanabe [c], Tomoko Kasahara [c], Tomomi Sudo [c], Fumihiko Shiota [c], Hirokuni Hashikata [e], Yasushi Takagi [e], Daisuke Morito [f], Susumu Miyamoto [e], Kazuwa Nakao [d], Akio Koizumi [a,*]

[a] Department of Health and Environmental Sciences, Kyoto University, Kyoto, Japan
[b] Radiation Biology Center, Kyoto University, Kyoto, Japan
[c] Center for iPS Cell Research and Application (CiRA), Kyoto University, Kyoto, Japan
[d] Department of Medicine and Clinical Science, Kyoto University, Kyoto, Japan
[e] Department of Neurosurgery, Kyoto University,Kyoto, Japan
[f] Faculty of Life Sciences, Kyoto Sangyo University, Kyoto, Japan

ARTICLE INFO

Article history:
Received 30 June 2013
Available online 12 July 2013

Keywords:
Moyamoya disease
iPS cells
Endothelium
Angiogenesis
RNF213
Securin

ABSTRACT

Moyamoya disease (MMD) is a cerebrovascular disease characterized by occlusive lesions in the circle of Willis. The RNF213 R4810K polymorphism increases susceptibility to MMD. Induced pluripotent stem cells (iPSCs) were established from unaffected fibroblast donors with wild-type RNF213 alleles, and from carriers/patients with one or two RNF213 R4810K alleles. Angiogenic activities of iPSC-derived vascular endothelial cells (iPSECs) from patients and carriers were lower (49.0 ± 19.4%) than from wild-type subjects ($p < 0.01$). Gene expression profiles in iPSECs showed that Securin was down-regulated ($p < 0.01$) in carriers and patients. Overexpression of RNF213 R4810K downregulated Securin, inhibited angiogenic activity (36.0 ± 16.9%) and proliferation of humanumbilical vein endothelial cells (HUVECs) while overexpression of RNF213 wild type did not. Securin expression was downregulated using RNA interference techniques, which reduced the level of tube formation in iPSECs and HUVECs without inhibition of proliferation. RNF213 R4810K reduced angiogenic activities of iPSECs from patients with MMD, suggesting that it is a promising *in vitro* model for MMD.

1. Introduction

Moyamoya disease (MMD) is an idiopathic cerebrovascular disease. It is characterized by occlusive lesions at the terminal portion of internal carotid arteries in the circle of Willis, with compensatory development of a fine vascular network that resembles "puffs of smoke" [1,2]. It is now recognized as one of the major causes of stroke in adults and children worldwide [3–6]. We recently identified *RNF213* as the susceptibility gene for MMD, and the p.R4810K (rs112735431, ss179362673: G>A; herein referred to as RNF213 R4810K) polymorphism as a founder variant commonly found in East Asian (Japanese, Korean and Chinese) patients [7]. RNF213 encodes a 591 kDa protein that exhibits ATPase and ubiquitin ligase activities. Although knockdown of RNF213 in zebrafish impaired angiogenesis, the physiological and biochemical functions of RNF213, and pathological consequences of MMD associated with RNF213 R4810K remain unknown [7].

The minor allele frequency of the founder RNF213 R4810K polymorphism in the general population is estimated to be 0.43–1.36% for East Asia, equivalent to a prevalence of 0.86–2.72% for carriers. RNF213 R4810K elevates the risk of MMD by more than 100-fold in carriers [7], with approximately 15 million individuals thought to be at extremely high risk [8]. The prevalence of patients with MMD (0.01%) is much lower than that for RNF213 R4810K carriers (3%) in Japan and Korea [3,4]. We have sought to determine the triggering factors that induce MMD in RNF213 R4810K carriers. Considering the social and economic dimensions of a large high-risk population in East Asia, determination of these MMD triggering

* Corresponding author. Address: Department of Health and Environmental Sciences, Graduate School of Medicine, Kyoto University, Konoe-cho, Yoshida, Sakyo-ku, Kyoto 606-8501, Japan. Fax: +81 75 753 4458.
E-mail address: koizumi.akio.5v@kyoto-u.ac.jp (A. Koizumi).
[1] These authors contributed equally to this work.

0006-291X/$ - see front matter © 2013 Elsevier Inc. All rights reserved.
http://dx.doi.org/10.1016/j.bbrc.2013.07.004

factors is a high-priority issue. Such triggers are considered to act through RNF213 R4810K, but elucidation of these triggers has been hampered, mainly because of the lack of knowledge with respect to RNF213 R4810K pathology.

The primary aims of our study were to characterize RNF213 R4810K and the physiological functions of RNF213. To determine the pathological defects attributable to RNF213 R4810K, we tested whether vascular endothelial cells from patients with MMD have lowered angiogenic activities. Our hypothesis was based on reports of defective angiogenic activities for circulating endothelial progenitor cells in MMD patients [9]. We used induced pluripotent stem cell (iPSC) technology with the hope that it might yield useful *in vitro* disease models [10]. This approach is particularly useful for diseases in which the pathological processes have yet to be elucidated. Once an *in vitro* model has been established it is possible to reveal pathological clues about a disease; it can then be employed as a drug-screening tool, paving the way for translational research. We characterized *ex vivo* phenotypes of vascular endothelial cells differentiated from iPSCs (iPSECs) and conducted a series of *in vitro* experiments to understand the underlying mechanisms of MMD.

2. Methods

2.1. Participants

We studied three probands from three unrelated families with MMD. Diagnosis was made based on criteria from the Japanese Research Committee on MMD (Ministry of Health, Labour and Welfare, Japan) [11]. Participants consisted of six affected, or unaffected and unrelated subjects (Table 1 and Supplementary data). Genotyping revealed a AA genotype (homozygous for RNF213 R4810K) for two affected subjects, a GA genotype (heterozygous for RNF213 R4810K) in one affected and one unaffected subject, and a GG genotype (wild-type for RNF213 R4810K) for two unaffected subjects. We obtained written informed consent from all participants in this study. Our study was approved by the Institutional Ethical Review Board of Kyoto University.

2.2. Establishment of iPSECs

Dermal fibroblasts were isolated from arms and cultured. Induction of iPSCs was performed as described previously (Supplementary data) from primary fibroblasts for three MMD patients, an unaffected carrier and two controls (Table 1). We then induced the differentiation of iPSCs into vascular endothelial cells (Supplementary data). Angiogenic activity of iPSECs was assayed by tube formation. Gene expression profiles were determined using a GeneChip microarray (Human Gene 1.0 ST; Supplementary data).

Table 1
Summary of donor fibroblast information.

ID	Diagnosis	Gender	Age at onset	Age at biopsy	R4810K (G>A) of RNF213
Control 1	Healthy control	F	NA	81	GG
Control 2	Healthy control	F	NA	6	GG
Unaffected carrier	Healthy control	M	NA	36	GA
Patient 1	Familial MMD	F	10	43	GA
Patient 2	Familial MMD	F	55	63	AA
Patient 3	Familial MMD	F	50	64	AA

MMD, moyamoya disease.

2.3. Cell culture and transfection

Fibroblasts were maintained in Dulbecco's Minimal Essential Medium (DMEM; Invitrogen, Tokyo, Japan) containing 10% fetal bovine serum (FBS; Japan Bioserum, Hiroshima, Japan). The iPSCs were maintained in Primate ES medium (ReproCELL, Tokyo, Japan) and supplemented with 500 U/ml penicillin/streptomycin (Invitrogen) and 4 ng/ml recombinant human basic fibroblast growth factor (bFGF; WAKO, Tokyo, Japan) as previously reported [10,12]. Human umbilical vein endothelial cells (HUVECs; Lonza, Walkersville, MD, USA) were maintained in EGM-2 (Lonza). An mCherry-tagged wild-type RNF213 or an mCherry-tagged RNF213 R4810K was cloned into pcDNA3.1 (Invitrogen) (Supplementary data). The plasmids were introduced with an Amaxa Nucleofector Device (Lonza).

2.4. Assessment of angiogenic activity

Endothelial tube formation was assessed as described previously [13]. The iPSECs (5000 cells/well) or HUVECs (5000 cells/well or 20,000 cells/well) were seeded onto matrigel-coated (BD Biosciences, Bedford, MA, USA) 96-well plates. Cells were incubated for 12 h at 37 °C and digital images of tubes that formed were captured. For quantitation, tube area, total tube length and the number of tube branches were calculated using Image J software (National Institute of Health, USA). Parameters for assessing tube formation function were obtained from three or four independent tube formation assays.

2.5. RNA interference (RNAi)

Transfection of small interfering RNAs (siRNAs) was conducted using Dharmafect (#1 or #3; Dharmacon, Lafayette, CO, USA) following the manufacturer's recommendations. We also used Nucleofector instruments to transfect HUVECs and iPSECs according to the manufacturer's protocols. We purchased and used Securin siRNA (sc-37491; Santa Cruz Biotechnology, Santa Cruz, CA, USA), RNF213 siRNA 1 (sc-94184; Santa Cruz Biotechnology) and RNF213 siRNA 2 (s33568; Ambion, Austin, TX, USA), with control siRNA-A (sc-37007, Santa Cruz Biotechnology) and silencer select negative control #1 siRNA (Ambion) used as controls. To monitor knockdown of gene expression, real-time quantitative polymerase chain reaction (qPCR), immunostaining and/or western blotting assays were conducted.

2.6. Growth curves

Cell proliferation was assessed using colorimetric 3,4,5-dimethylthiazol-2-yl-2,5-diphenyl tetrazolium bromide (MTT) assays, which were carried out as described previously [14] unless otherwise specified. For growth curves for HUVECs in the overexpression experiment of RNF213 wild type and R4810K, at 2 days post-transfection, HUVECs were re-seeded at a density of 8×10^4 -cells/3.5-mm dish. Viable cells were assessed and counted each day using trypan blue (Nacalai Tesque) exclusion.

2.7. Western blotting

We used the CelLytic M (Sigma–Aldrich, St Louis, MO, USA) cell lysis buffer containing a protease inhibitor cocktail (Nacalai Tesque). In certain cases we also used a lysis buffered comprising 50 mM Tris–HCl (pH 8.0), 1% Nonidet P-40 and 150 mM NaCl. Samples were subjected to immunoblotting using the anti-RNF213

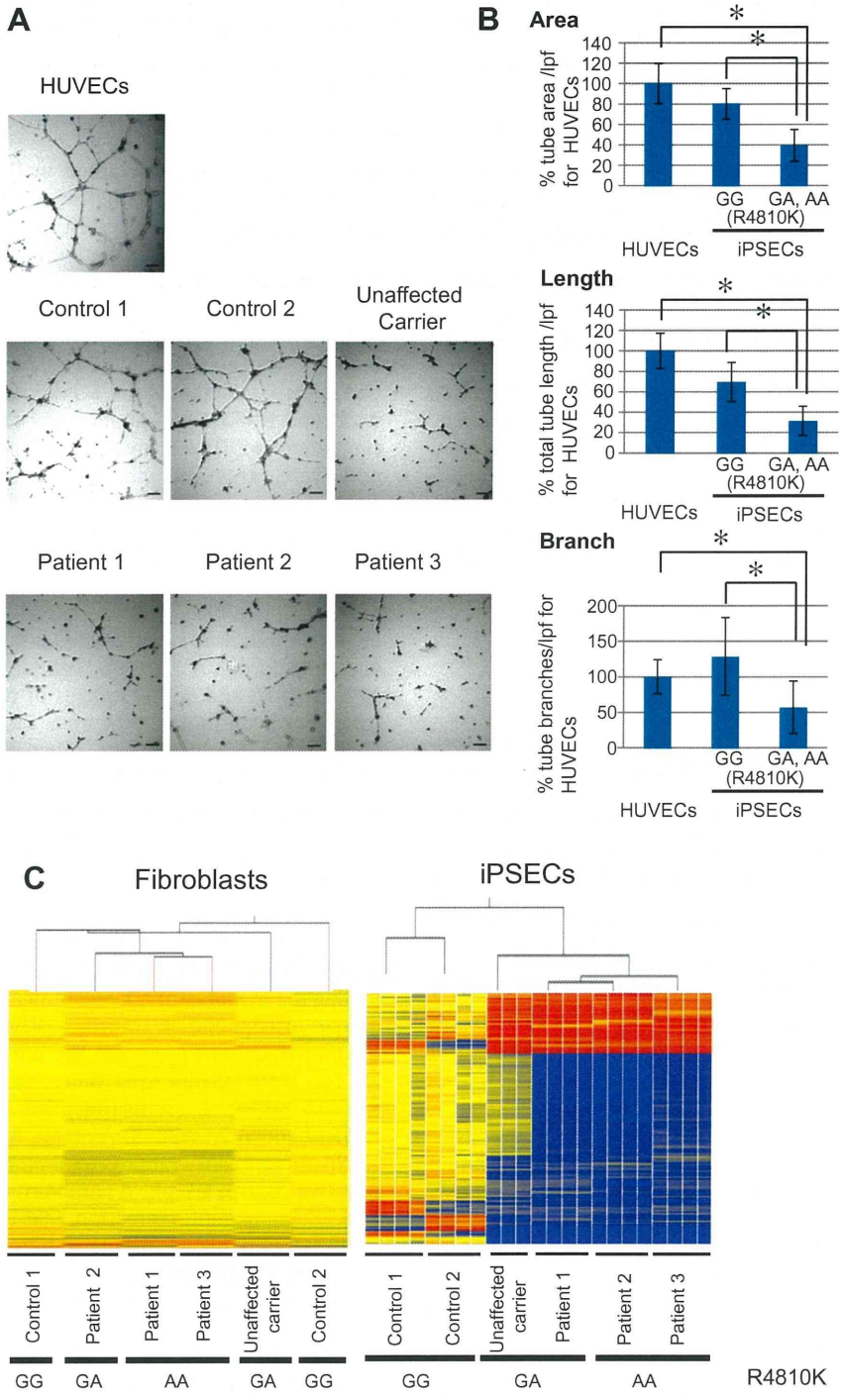

Fig. 1. Reduced angiogenic activities and differential gene expression in iPSECs. (A) Representative photomicrographs show the formation of tube-like structures in HUVECs and iPSECs from controls (GG genotype), the unaffected carrier, and patients (GA or AA genotypes). The scale bar indicates 100 μm. (B) Tube area, length and branch per low power field (lpf) were determined by matrigel assays and imaging analysis ($n = 3–4$, $^*p < 0.05$ using Student's t-test). Quantitative analysis of tube formation for iPSECs was performed between the GG genotype, and the GA and AA genotypes of p.R4810K on RNF213. HUVECs were used as a positive control. (C) Cluster analysis of fibroblasts from the control, unaffected carrier and MMD patients (single experiment) using microarrays (left panel). Cluster analysis of iPSECs from the unaffected carrier (three independent experiments), control and MMD patients (four independent experiments) using microarrays (right panel). Differentially regulated genes that were identified have been presented in Table S1.

antibody, which we generated (Supplementary data), or using anti-Securin (PTTG; Zymed, San Francisco, CA, USA), anti-β-tubulin (Sigma–Aldrich) or anti-β-actin (Abcam, Cambridge, UK) antibodies. Quantitation was conducted using Image J software.

2.8. Statistical analysis

Results are presented as the mean ± standard deviation (SD). Differences between groups were analyzed using analysis of variance (ANOVA), followed by Tukey's honestly significant difference

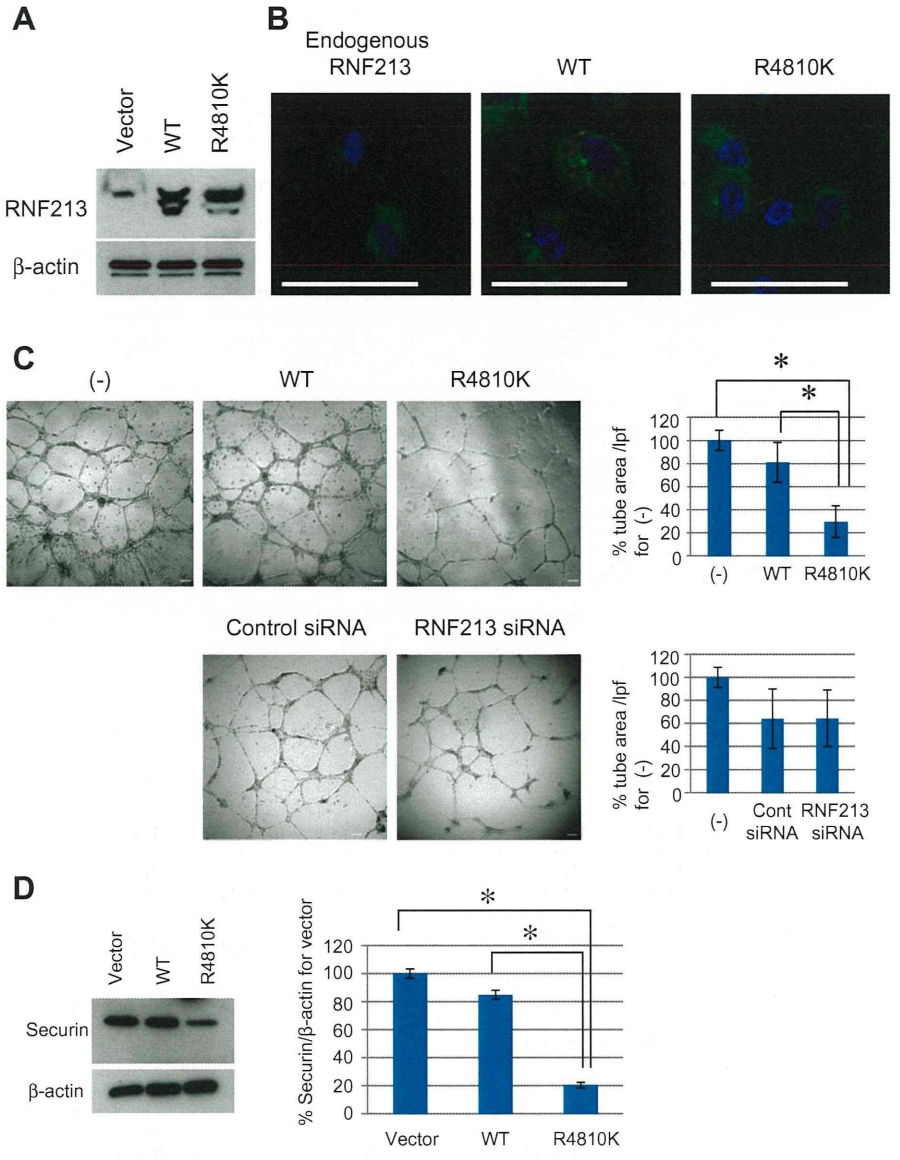

Fig. 2. Effects of RNF213 R4810K overexpression on the angiogenic activities of HUVECs. (A) Western blot analysis of endogenous and exogenous RNF213 in HUVECs. β-Actin was used as a loading control for all Western blots. (B) Subcellular localization of exogenous wild-type RNF213-mCherry (WT), RNF213 R4810K-mCherry (R4810K) and endogenous RNF213 in HUVECs. Left panel: HUVECs were stained for RNF213 (green) and DNA (blue). Middle and right panels: HUVECs transfected with RNF213-mCherry (red) were stained for tubulin (green) and DNA (blue). (C) Tube formation assays for HUVECs transfected with the RNF213 expression vector or RNF213 siRNA after 12 h of culture on matrigel. Non-transfected HUVECs (−) were used as a positive control. The scale bar indicates 100 μm. The tube areas for RNF213 overexpression ($n = 4$, $^*p < 0.05$ using Student's t-test) and siRNAs ($n = 3$) were quantified (right panel). Similar results were obtained for length and branch (data not shown). (D) Western blot analysis of Securin in HUVECs overexpressing wild-type RNF213 and RNF213 R4810K, with β-actin used as a loading control ($^*p < 0.01$ using Student's t-test). Data represents the mean of at least three independent experiments. (For interpretation of the references to color in this figure legend, the reader is referred to the web version of this article.)

test for comparisons involving more than two means (SAS Institute Inc., Cary, NC, USA). A p-value less than 0.05 was considered statistically significant.

3. Results

3.1. iPS cell clones

We established iPSCs from three unaffected subjects and three patients with MMD (Table 1). We used qPCR to select iPSC clones where exogenously introduced genes were repressed (Fig. S1A). Genetic identity was confirmed by genotypes of short tandem repeat (STR) markers between donor fibroblasts and iPSCs derived from these cells (Fig. S1B). All six iPSC clones showed characteristics of human embryonic stem cell morphology. They also expressed pluripotency markers, including NANOG, OCT4, SOX2, SSEA4, TRA-1-60, TRA-1-81 and alkaline phosphatase (ALP) enzymatic activity (Fig. S1C). We confirmed that there was no expression of SSEA1. The pluripotent properties of the iPSCs were confirmed by examining methylation of the OCT4 and NANOG promoter regions (Fig. S1D), and by embryoid body (EB) formation (Fig. S1E).

3.2. Reduced angiogenic activities of iPSECs in subjects with RNF213 R4810K

The iPSECs derived from iPSCs showed typical morphological features. They exhibited a cobblestone-like appearance on culture dishes, and expressed eNOS, CD31, VE-Cadherin, vWF and CD34, while iPSCs did not (Fig. S2C and D). All these features correspond

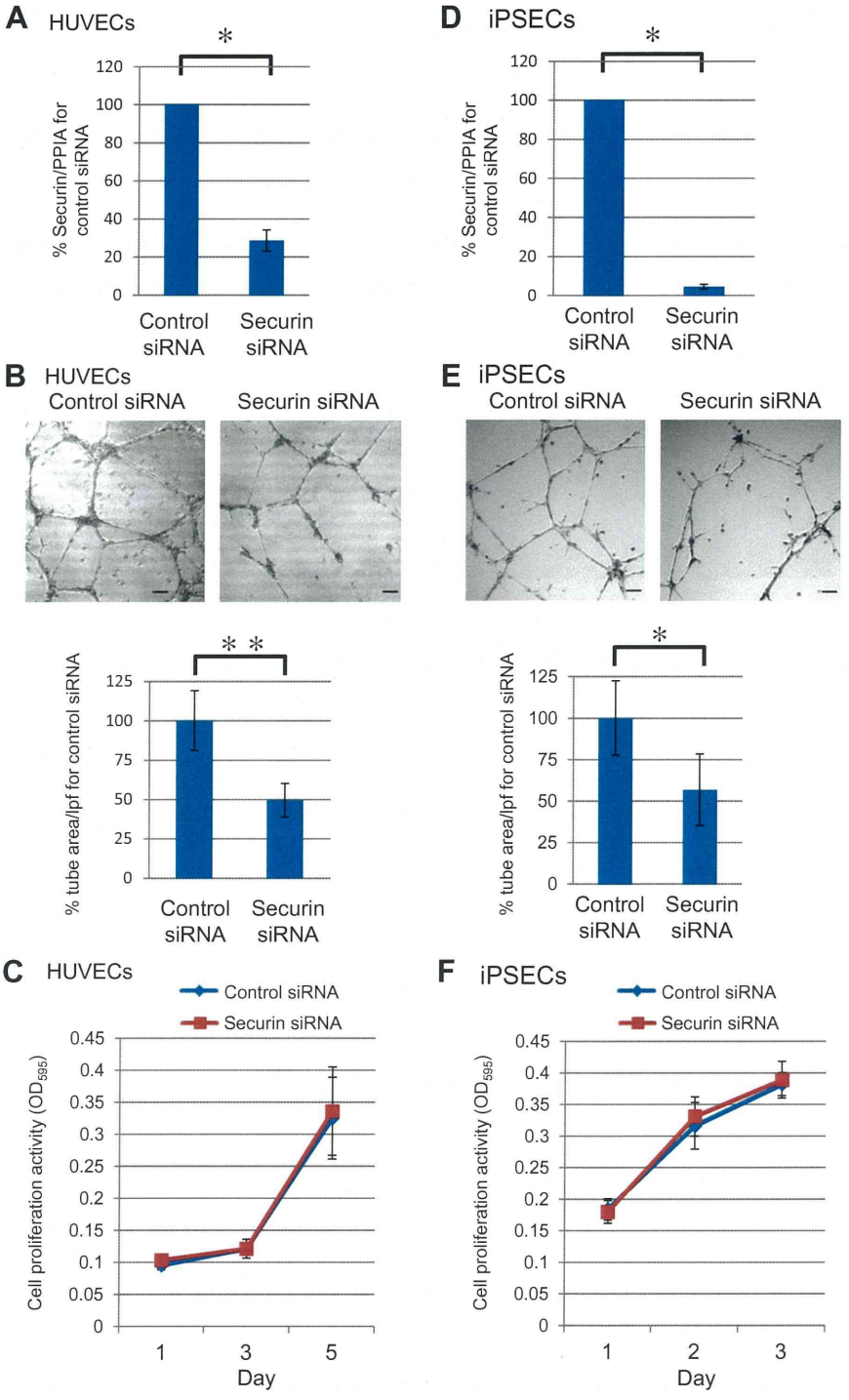

Fig. 3. The effect of depletion of Securin on angiogenic activities in HUVECs and iPSECs from a control subject. (A) RNA levels of Securin in HUVECs treated with control and Securin siRNA ($n = 3$, $^{*}p < 0.05$ using Student's t-test). (B) Representative photomicrographs (upper) and tube areas per low power field (lpf) (lower) of HUVECs treated with control and Securin siRNA ($n = 3$, $^{**}p < 0.01$ using Student's t-test). Similar results were obtained for length and branch (data not shown). The scale bar indicates 100 μm. (C) Time course of cell proliferation for HUVECs treated with control and Securin siRNA. (D) RNA levels of Securin in control iPSECs treated with control and Securin siRNA ($n = 3$, $^{*}p < 0.05$ using Student's t-test). (E) Representative photomicrographs (upper) and tube areas per lpf (lower) of control iPSECs treated with control and Securin siRNA ($n = 3$, $^{*}p < 0.05$ using Student's t-test). Similar results were obtained for length and branch (data not shown). The scale bar indicates 100 μm. (F) Time course of cell proliferation for control iPSCs treated with control and Securin siRNA.

to characteristics of vascular endothelial cells. We investigated iPSEC angiogenic activity by tube formation. The iPSECs from MMD patients and an unaffected carrier revealed significantly reduced tube areas compared with those from controls (wild-type RNF213; Fig. 1A and B and Fig. S3). Lower angiogenic activity was also confirmed by total tube length and numbers of branches (Fig. 1A and B, Fig. S3), but could not be attributed to the suppression of growth (Fig. S4).

3.3. Downregulation of mitotic phase-associated genes in iPSECs with RNF213 R4810K

To better understand whether RNF213 R4810K affects expression levels of specific genes related to reduced angiogenic activity, we used microarrays to identify differentially expressed genes in iPSECs and their parental fibroblasts. Cluster analysis of expression profiles demonstrated a clear difference for iPSECs with the RNF213 R4810K genotype (Fig. 1C).

In the iPSECs, the expression levels of 159 genes were differentially regulated by more than three-fold ($p < 0.01$). Our analysis revealed that 38 genes were up-regulated, and 121 were down-regulated (Table S1). Gene ontology analysis identified 161 significant terms ($p < 0.01$; Tables S2). Gene and ontology classifications revealed that many mitotic phase-associated genes were down-regulated (Tables S1 and S2) in iPSECs from donors with the RNF213 R4810K polymorphism. We confirmed the microarray results through qPCR assays for five genes (*Securin*, *BUB1*, *NDC80*, *PLK1* and *CDC20*) (Fig. S5).

3.4. Effects of RNF213 R4810K overexpression

Wild-type RNF213 and/or RNF213 R4810K proteins fused to the mCherry reporter (Fig. S6) were overexpressed in HUVECs (Fig. 2A and B). Plasmids were transfected into HUVECs by electroporation with gene transfer efficiencies around 72%. Overexpression of RNF213 R4810K reduced angiogenic activity in HUVECs (Fig. 2C) and significantly inhibited proliferation of HUVECs (Fig. S8). In contrast, neither overexpression nor depletion of wild-type RNF213 reduced angiogenic activity (Fig. 2C) or proliferation (Fig. S8). Localization of exogenous RNF213 R4810K was similar to that for the exogenous and endogenous wild-type RNF213, with these proteins observed in the cytoplasm around the nucleus (Fig. 2B). Overexpression of RNF213 R4810K significantly down-regulated the expression of Securin ($p < 0.01$; Fig. 2D), while overexpression of wild-type RNF213 had little effect on Securin.

3.5. Depletion of Securin affects angiogenic activities of HUVECs and iPSECs

Securin induces angiogenesis, and is an inhibitor of premature sister chromatid separation [15]. Depletion of Securin induces severe defects in cell migration by lowered microtubule nucleation [16], which results in lowered angiogenic activity. We then examined the effects of RNAi-mediated depletion of Securin on tube formation and proliferation using HUVECs and iPSECs carrying wild alleles. RNAi knockdown of Securin was shown to impair tube formation without inhibiting proliferation in both HUVECs (Fig. 3A–C) and iPSECs (Fig. 3D–F).

4. Discussion

In this study, we successfully differentiated iPSECs from the iPSCs of MMD patients and carriers harboring GA or AA genotypes of RNF213 R4810K. The iPSECs with GA or AA genotypes replicated lowered angiogenic activity for circulating endothelial progenitor cells in MMD patients [9]. To the best of our knowledge, we are the first to report the generation of MMD-specific iPSCs that are able to differentiate into iPSECs, which can then be used as an *in vitro* MMD model.

Reduced angiogenic activity was consistently observed in iPSECs from subjects that had RNF213 R4810K, and in HUVECs overexpressing RNF213 R4810K. Because gene expression of Securin, which is known to require for angiogenesis [15], was suppressed in iPSECs carrying RNF213 R4810K, we investigated the effects of RNAi-mediated knockdown of Securin on tube formation in HUVECs and iPSECs. Depletion of Securin inhibited tube formation consistently without inhibition of proliferation as we observed lowered tube formation of iPSECs from patients and the carrier. This indicated to us that reduced expression of Securin per se is responsible for lowered angiogenic activity. Because cell migration is known to be impaired when Securin is depleted [16], we postulate that the defect in migration might occur in iPSECs, thereby reducing angiogenic activity.

We did not investigate abnormalities of vascular smooth muscle cells (VSMCs), which could be considered a limitation of our work. A major pathological finding in MMD is the excessive proliferation of VSMCs. The interactions between ECs and VSMCs are known to play key roles in vascular structure and function of vessels. VSMC migration, proliferation, and differentiation are critical processes involved in intimal hyperplasia and are under regulation by endothelial cells [17]. We postulate that there is a defect in the crosstalk between ECs and VSMCs in patients.

Many mitosis-related genes were downregulated by RNF213 R4810K. We focused on Securin and determined that its downregulation may play a substantial role in lowered angiogenic activity of iPSECs from patients with MMD. However, in the present study, we did not investigate the effects of other downregulated genes. Furthermore, we did not investigate the mechanisms of Securin downregulation in iPSECs from MMD patients. Further studies are needed to substantiate the roles of RNF213 R4810K in downregulation of mitotic associated genes.

In conclusion, we observed that iPSECs from MMD patients had impaired angiogenic functions. RNF213 R4810K manifests as defects in angiogenesis by the downregulation of Securin expression. The resulting defects in angiogenesis are considered risk factors for MMD patients. Furthermore, our study demonstrated that iPSECs can serve as an *in vitro* MMD model, as they express a useful benchmark phenotype for high throughput screening, which can be applied to drug development and discovering MMD triggers.

Funding sources

This work was supported by grants from the Ministry of Education, Culture, Sports, Science and Technology of Japan (Nos. 17109007 and 22249020 to Dr. Koizumi). This research was partially supported by the Japan Society for the Promotion of Science through its Funding Program for World-Leading Innovative R&D on Science and Technology (FIRST Program to Dr. Osafune).

Acknowledgments

We are grateful to Drs. Wanyang Liu, Shanika Nanayakkara, and STMLD Senevirathna (Kyoto University Graduate School of Medicine) for their technical support.

Appendix A. Supplementary data

Supplementary data associated with this article can be found, in the online version, at http://dx.doi.org/10.1016/j.bbrc.2013.07.004.

References

[1] J. Suzuki, A. Takaku, Cerebrovascular "moyamoya" disease. Disease showing abnormal net-like vessels in base of brain, Arch. Neurol. 20 (1969) 288–299.
[2] K. Takeuchi, K. Shimizu, Hypogenesis of bilateral internal carotid arteries, Brain Nerve 9 (1957) 37–43.
[3] S. Kuroda, K. Houkin, Moyamoya disease: current concepts and future perspectives, Lancet Neurol. 7 (2008) 1056–1066.
[4] W. Miao, P.L. Zhao, Y.S. Zhang, H.Y. Liu, Y. Chang, J. Ma, Q.J. Huang, Z.X. Lou, Epidemiological and clinical features of moyamoya disease in Nanjing, China, Clin. Neurol. Neurosurg. 112 (2010) 199–203.

[5] R.M. Scott, E.R. Smith, Moyamoya disease and moyamoya syndrome, N. Engl. J. Med. 360 (2009) 1226–1237.
[6] A. Veeravagu, R. Guzman, C.G. Patil, L.C. Hou, M. Lee, G.K. Steinberg, Moyamoya disease in pediatric patients: outcomes of neurosurgical interventions, Neurosurg. Focus 24 (2008) E16.
[7] W. Liu, D. Morito, S. Takashima, Y. Mineharu, H. Kobayashi, T. Hitomi, H. Hashikata, N. Matsuura, S. Yamazaki, A. Toyoda, K. Kikuta, Y. Takagi, K.H. Harada, A. Fujiyama, R. Herzig, B. Krischek, L. Zou, J.E. Kim, M. Kitakaze, S. Miyamoto, K. Nagata, N. Hashimoto, A. Koizumi, Identification of RNF213 as a susceptibility gene for moyamoya disease and its possible role in vascular development, PLoS ONE 6 (2011) e22542.
[8] W. Liu, T. Hitomi, H. Kobayashi, K.H. Harada, A. Koizumi, Distribution of moyamoya disease susceptibility polymorphism p.R4810K in RNF213 in East and Southeast Asian Populations, Neurol. Med. Chir. 52 (2012) 299–303.
[9] J.H. Kim, J.H. Jung, J.H. Phi, H.S. Kang, J.E. Kim, J.H. Chae, S.J. Kim, Y.H. Kim, Y.Y. Kim, B.K. Cho, K.C. Wang, S.K. Kim, Decreased level and defective function of circulating endothelial progenitor cells in children with moyamoya disease, J. Neurosci. Res. 88 (2010) 510–518.
[10] K. Takahashi, K. Tanabe, M. Ohnuki, M. Narita, T. Ichisaka, K. Tomoda, S. Yamanaka, Induction of pluripotent stem cells from adult human fibroblasts by defined factors, Cell 131 (2007) 861–872.
[11] M. Fukui, Guidelines for the diagnosis and treatment of spontaneous occlusion of the circle of Willis ('moyamoya' disease). Research Committee on Spontaneous Occlusion of the Circle of Willis (Moyamoya Disease) of the Ministry of Health and Welfare, Japan, Clin. Neurol. Neurosurg. 99 (Suppl. 2) (1997) S238–S240.
[12] K. Amps, P.W. Andrews, G. Anyfantis, L. Armstrong, S. Avery, H. Baharvand, J. Baker, D. Baker, M.B. Munoz, S. Beil, N. Benvenisty, D. Ben-Yosef, J.C. Biancotti, A. Bosman, R.M. Brena, D. Brison, G. Caisander, M.V. Camarasa, J. Chen, E. Chiao, Y.M. Choi, A.B. Choo, D. Collins, A. Colman, J.M. Crook, G.Q. Daley, A. Dalton, P.A. De Sousa, C. Denning, J. Downie, P. Dvorak, K.D. Montgomery, A. Feki, A. Ford, V. Fox, A.M. Fraga, T. Frumkin, L. Ge, P.J. Gokhale, T. Golan-Lev, H. Gourabi, M. Gropp, G. Lu, A. Hampl, K. Harron, L. Healy, W. Herath, F. Holm, O. Hovatta, J. Hyllner, M.S. Inamdar, A.K. Irwanto, T. Ishii, M. Jaconi, Y. Jin, S. Kimber, S. Kiselev, B.B. Knowles, O. Kopper, V. Kukharenko, A. Kuliev, M.A. Lagarkova, P.W. Laird, M. Lako, A.L. Laslett, N. Lavon, D.R. Lee, J.E. Lee, C. Li, L.S. Lim, T.E. Ludwig, Y. Ma, E. Maltby, I. Mateizel, Y. Mayshar, M. Mileikovsky, S.L. Minger, T. Miyazaki, S.Y. Moon, H. Moore, C. Mummery, A. Nagy, N. Nakatsuji, K. Narwani, S.K. Oh, C. Olson, T. Otonkoski, F. Pan, I.H. Park, S. Pells, M.F. Pera, L.V. Pereira, O. Qi, G.S. Raj, B. Reubinoff, A. Robins, P. Robson, J. Rossant, G.H. Salekdeh, T.C. Schulz, et al., Screening ethnically diverse human embryonic stem cells identifies a chromosome 20 minimal amplicon conferring growth advantage, Nat. Biotechnol. 29 (2011) 1132–1144.
[13] M. Potente, L. Ghaeni, D. Baldessari, R. Mostoslavsky, L. Rossig, F. Dequiedt, J. Haendeler, M. Mione, E. Dejana, F.W. Alt, A.M. Zeiher, S. Dimmeler, SIRT1 controls endothelial angiogenic functions during vascular growth, Genes Dev. 21 (2007) 2644–2658.
[14] T. Mosmann, Rapid colorimetric assay for cellular growth and survival: application to proliferation and cytotoxicity assays, J. Immunol. Methods 65 (1983) 55–63.
[15] H. Ishikawa, A.P. Heaney, R. Yu, G.A. Horwitz, S. Melmed, Human pituitary tumor-transforming gene induces angiogenesis, J. Clin. Endocrinol. Metab. 86 (2001) 867–874.
[16] M.A. Moreno-Mateos, A.G. Espina, B. Torres, M.M. Gamez del Estal, A. Romero-Franco, R.M. Rios, J.A. Pintor-Toro, PTTG1/securin modulates microtubule nucleation and cell migration, Mol. Biol. Cell 22 (2011) 4302–4311.
[17] F. Milliat, A. Francois, M. Isoir, E. Deutsch, R. Tamarat, G. Tarlet, A. Atfi, P. Validire, J. Bourhis, J.C. Sabourin, M. Benderitter, Influence of endothelial cells on vascular smooth muscle cells phenotype after irradiation: implication in radiation-induced vascular damages, Am. J. Pathol. 169 (2006) 1484–1495.